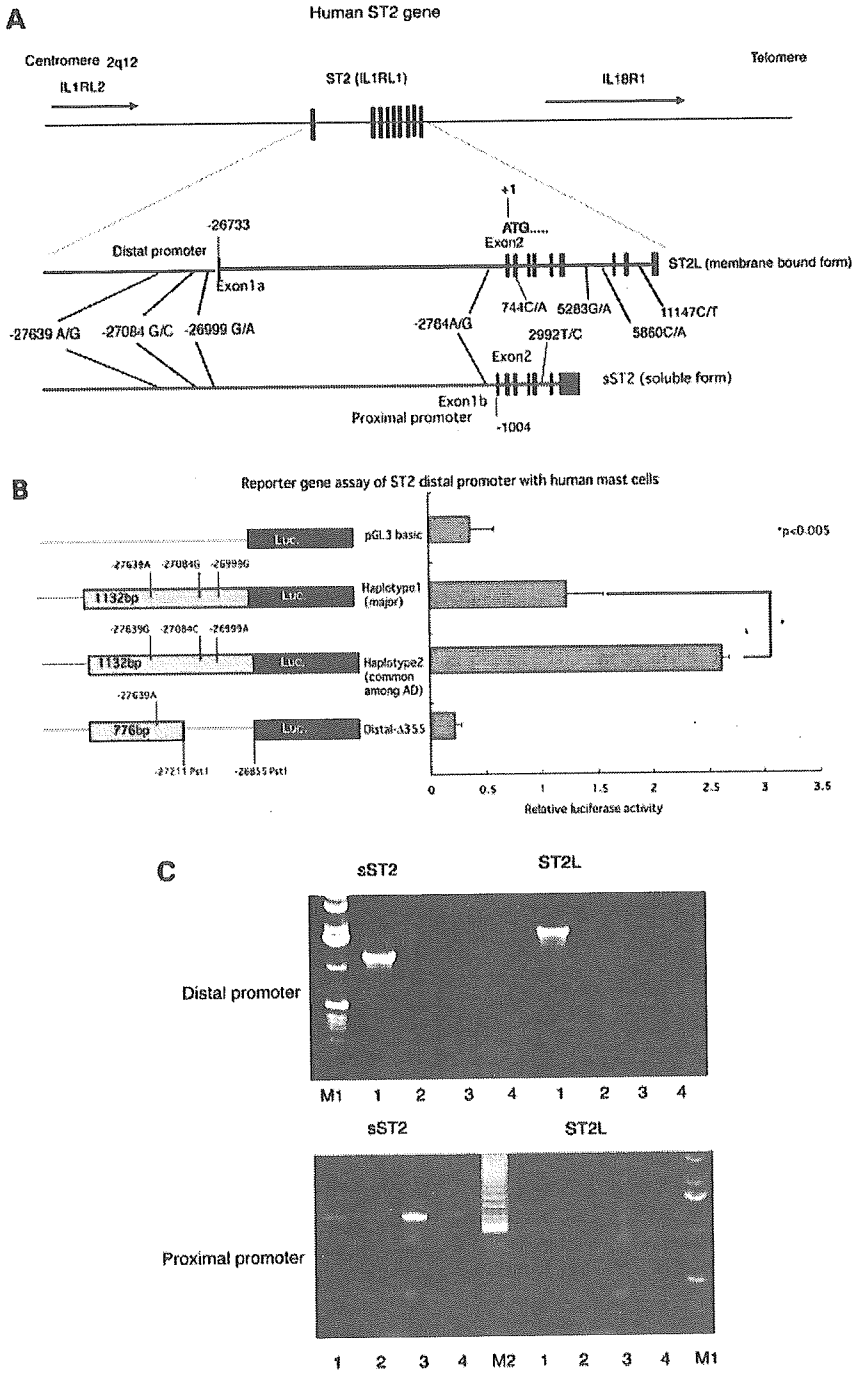

Figure 1. *ST2* gene structures and the roles of promoters in the induction of ST2 transcripts. (A) ST2 (IL1RL1) locus SNP map in the genomic region. The complete coding region of ST2, intron/exon boundaries, ~3 kb of 5′-genomic DNA, is shown. The longer variant (ST2L) has 11 exons and the shorter variant (sST2) has eight exons. These exons are indicated by closed rectangles. (**B**) Comparison of allelic variants of the ST2 distal promoter region analyzed by luciferase activity. Allelic differences in luciferase activity were examined using human mast (LAD2) cells. The constructs of the reporter plasmids are shown on the left. Five hundred nanograms of each plasmid was transfected with 10 ng of pRL-TK vector. Transcriptional activity was determined by assaying the *firefly* luciferase activity of cellar extracts prepared 24 h after transfection. Data show the mean ± SD relative activity from a representative experiment done in triplicate. $^*P = 0.004$ by Student's *t*-test. (**C**) RT–PCR with cDNA from various cells in skin using specific primer sets for distinguishing each promoter and subtype (ST2L/sST2) expression. (Top left) Forward primer: exon 1a (distal promoter), reverse primer: sST2 specific region. (Top right) Forward: exon 1a, reverse: ST2L-specific region. (Bottom left) Forward: exon 1b (proximal promoter), reverse: sST2. (Bottom right) Forward: exon 1b, Reverse: ST2L. Lane 1: LAD2 (mast cells), lane 2: KC cultured with serum-free medium (SFM), lane 3: KC cultured with SFM + 10% FBS for 24 h, lane 4: dermal fibroblasts. M1: 1 kb molecular marker, M2: 100 bp molecular marker.

Table 1. Genotype frequencies for ST2 SNPs and AD susceptibility

	SNP number	Location	Control ($n = 636$)					AD ($n = 452$)					*P*-value[a]	*P*-value[b]	*P*-value[c]
			1	2	3	Sum	Minor allele frequency	1	2	3	Sum	Minor allele frequency			
1	14	−27639A/G	205	295	124	624	0.44	99	235	115	449	0.52	0.0026[d]	0.0007[d]	NS
2	18	−26999G/A	223	279	112	614	0.41	106	240	106	452	0.50	0.00024[d]	0.000049[d]	NS
3	41	744C/A	415	182	28	625	0.19	313	123	9	445	0.16	NS	NS	NS
4	49	2992C/T	221	286	113	620	0.41	183	205	57	445	0.36	NS	NS	NS
5	51	5283G/A	272	273	79	624	0.35	204	195	48	447	0.33	NS	NS	NS
6	57	5860C/A	225	284	110	619	0.41	187	205	56	448	0.35	NS	NS	NS
7	67	11147C/T	251	280	91	622	0.37	209	189	47	445	0.32	NS	NS	NS

NS, not significant.
[a]Allele1 versus allele2.
[b]Genotype11 versus 12 + 22.
[c]Genotype11 + 12 versus 22.
[d]*P*-value statistically significant after Bonferroni correction (raw *P*-values were multiplied by 7).

Table 2. Association between ST2-26999 G/A SNP and AD

	Controls ($n = 614$)	AD ($n = 452$)	χ^2 (*P*-value)	OR (95% CI)	AD total IgE>1700 ($n = 290$)	χ^2 (*P*-value)	OR (95% CI)
−26999G/A			GG:others			GG:others	
GG	223	106	20.20	1.86	53	30.23	2.55
GA	279	240	(0.0000070)[a]	(1.42–2.45)	166	(0.000000038)[a]	(1.81–3.58)
AA	112	106	(0.000049)[b]		71	(0.00000027)[b]	

[a]Raw *P*-value.
[b]*P*-value after Bonferroni correction.

Table 3. Haplotype structures and frequencies in ST2 distal promoter

Haplotype −27639, −26999	Haplotype frequency Case	Control	χ^2	*P*-value	OR
A, G	0.56	0.48	13.00	0.0012	1.37
G, A	0.41	0.50	15.14	0.0004	1.41
G, G	0.025	0.019	0.85	0.35	1.32

two separate experiments and the results were similar. The total IgE concentration in the sera of 428 AD patients was measured with the fluorescence-enzyme immunoassay (FEIA) (Supplementary Material, Fig. S4B). The total IgE concentrations were 5371.9 IU/ml (mean) for the sera from −26999G/G genotype patients and 7898.7 IU/ml for those from −26999 G/A + A/A genotype patients. The serum concentration of total IgE was significantly lower in the sera of −26999G/G patients ($P = 0.0024$ by Mann–Whitney *U*-test). The correlation between the sST2 and the total IgE concentration was examined among −26999A/A genotype patients (Supplementary Material, Fig. S4C); Pearson's correlation coefficient was 0.28.

ST2L protein expression on the surface of human mast cells

Immunoprecipitation (IP) and subsequent western blotting using LAD2 cell lysate showed a positive band around 90 kDa in the IP samples with an anti-ST2 antibody (clone2A5). Deglycosylation with PNGaseF showed a shift of the band to lower molecular weight, corresponding to the molecular weight of non-glycosylated ST2L protein (Fig. 2A). To further demonstrate the surface expression of ST2L protein, non-stimulated LAD2 cells were stained with the anti-ST2 antibody (with FITC) and analyzed by FACS. The histogram showed a positive shift of the mean FITC intensity of ST2 staining (dotted line, Fig. 2B) compared with that of isotype-matched mouse IgG.

Immunohistochemistry

A paraffin section of the skin biopsy sample from an AD patient in the acute stage was stained with an anti-ST2 monoclonal antibody (clone HB12). Positive staining was observed on the cell surface of KC in the suprabasal layer and infiltrating cells in the dermal layer (Fig. 3A and C). ST2-positive staining was observed only with the infiltrating cells in the dermal layer of the skin of another AD patient in the chronic stage (Fig. 3B). Immunostaining with control mouse IgG_1 did not show positive signals (data not shown).

DISCUSSION

We found an SNP in the distal promoter region of ST2 (−26999G/A) that showed a significant association with AD during our series of genetic association studies within the IL1R gene cluster. This is the first association study for the

Table 4. Haplotype structures and frequencies in ST2

HaplotypeID	Haplotype frequency		−27639	−26999	744	2992	5283	5860	11147
	Case	Control							
Haplotype A	0.41	0.5	G	A	C	T	A	C	C
Haplotype B	0.33	0.32	A	G	C	C	G	A	T
Haplotype C	0.13	0.12	A	G	A	T	A	C	C

Haplotype1/others: $\chi^2 = 17.5$; $P = 0.000028$; OR = 1.45.
Haplotype2/others: $\chi^2 = 0.15$; $P = 0.703$; OR = 1.04.
Haplotype3/others: $\chi^2 = 0.57$; $P = 0.451$; OR = 1.1.

ST2 gene and the results are intriguing, because the SNPs directly affect the expression level of Th2 cell marker ST2. Recent studies have clearly shown essential functional roles of ST2L protein for Th2-mediated immune responses (13,18,19), so it seems reasonable to investigate ST2 genetic polymorphism as a candidate for conferring susceptibility to AD. The result of case–control association studies of seven representative SNPs (Table 1) and haplotype analysis (Tables 3 and 4) showed that the highest association with AD was observed with the −26999G/A SNP as a single locus. There were four other SNPs in the ST2 genomic region that showed tight LD with the −26999G/A SNP. Three SNPs were located distal to the −26999G/A SNP in the distal promoter region. Two SNPs (−28214T/C; 3258 bp distal from the transcription starting site and −29778C/A; 1694 bp distal from the site) were not included in the functional analysis because our series of 5′-deletion promoter assays showed that the critical region for ST2 distal promoter activity was located within 300–500 bp from the transcriptional starting point (20); therefore, these two SNPs seemed to be less functional. Of the remaining two SNPs, one SNP (−27084G/C) was located at 85 bp distal to the −26999G/A SNP (236 bp distal to the transcriptional starting site); therefore, we decided to analyze these two SNPs together by reporter gene assay. The last SNP (−2874A/G) in tight LD with −26999G/A, located in the proximal promoter region of the *ST2* gene, did not affect the proximal promoter activity (Supplementary Material, Fig. S2).

The distal promoter reporter gene assay was performed with two 1132 bp distal promoter constructs, including two major haplotypes −27639A/−27084G/−26999G and −27639G/−27084C/−26999A covering >97% of haplotype frequency (Table 3). In addition to the two SNPs in the state of complete LD, (−27084/−26999), another SNP (−27639 A/G) that also showed a weak association with AD (Table 1) was included for analysis. We have reported that a GATA element commonly observed in both human and mouse *ST2* gene distal promoter region was indispensable for the activation of the promoter activity in Th2 cells (20,21). Therefore, we made another set of promoter assay constructs (Distal-Δ355) deprived of the GATA binding site and two SNP sites, which showed abrogated transcriptional activity (Fig. 1B). From these results, we concluded that this 356 bp region was essential for ST2 transcription and that the two SNPs (−27084G/C and −26999G/A) had major influences on the distal promoter activity among the SNPs with significant associations.

For further analysis of the roles of the genetic polymorphisms, we measured the serum concentrations of sST2 and total IgE and sorted the results by the genotype in the distal promoter. As the association study showed the most significant result under a dominant model (Tables 1 and 2), we compared the results by the genotype −26999G/G (low risk for AD) versus −26999A/G + A/A (high risk for AD). The results matched the results of the reporter gene assay and the association study. Furthermore, the genetic association between the −26999G/A SNP and AD patients for very high serum total IgE (IgE > 1700 IU/ml) became stronger (Table 2). These results suggested that having at least one allele of −26999A was correlated with a high sST2 level and a high total IgE concentration and an increased risk for AD. There is some controversy over the role of IgE in the pathogenesis of AD (22); therefore, it will be useful to genotype intrinsic AD (1) patients in the future.

We found a weak correlation ($r = 0.28$) between the serum sST2 level and the total IgE concentration with the genotype −26999AA patients. This finding was consistent with the recent report that the increase of food-specific IgE is paralleled by elevated sST2 levels, not by serum IL-4, IL-13 and interferon gamma levels (23). These results suggested possible effects of sST2 in IgE production, so further studies seem to be essential.

We reported sST2 concentrations of 200 healthy controls and 56 asthmatic patients previously (24). The sST2 concentration of healthy controls was 0–1.65 ng/ml (mean 0.415 ng/ml) and that of asthmatic patients was 0–2.40 ng/ml (mean 0.493 ng/ml). A differential rise of the serum ST2 level that correlated well with the severity of asthma exacerbation was observed (24). The serum concentration of sST2 in AD patients [0–1.02 ng/ml (mean 0.326 ng/ml)] was not significantly higher or lower than that of healthy controls or asthmatics; nonetheless, there was a correlation between the ST2 genotype and the sST2 concentration. We are now investigating the changes of the sST2 concentration during the clinical stages of AD, and the results might further clarify the role of sST2 in AD.

It has been reported that the usage of two different promoters (distal and proximal) depends on the type of cell for the human *ST2* gene (21). Consistent with this report, we showed that only hematopoietic cells utilized the distal promoter and that ST2 transcription of other skin cells (KC, dermal fibroblasts) was initiated from the proximal promoter (Fig. 1C). These results suggested that the significant association of SNPs −27084 and −26999 in the ST2 distal promoter

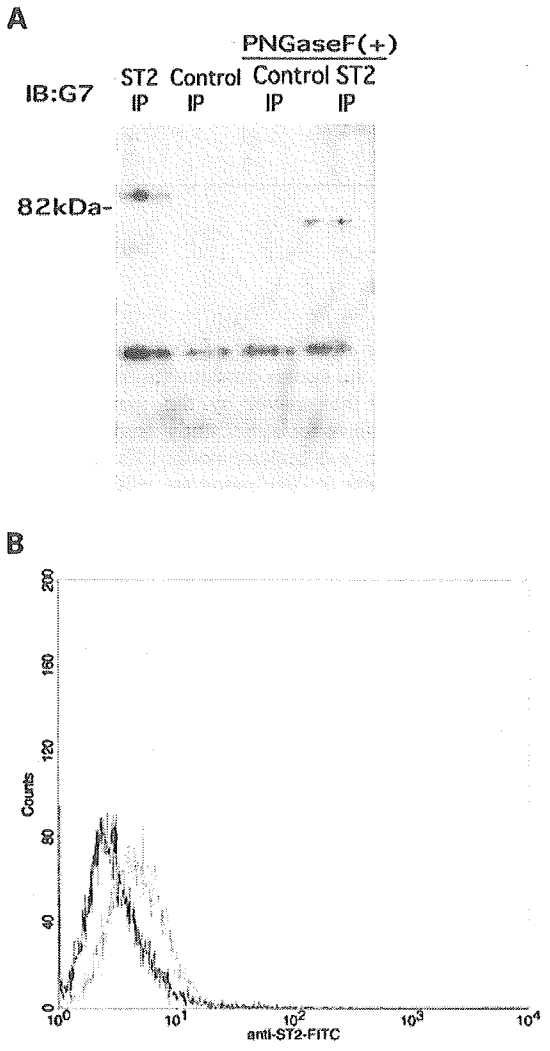

Figure 2. ST2L expression in LAD2 cells. (**A**) LAD2 cell lysate samples were immunoprecipitated with either an anti-ST2 IgG antibody (2A5) or an isotype-matched control antibody. The immunoprecipitated samples were electrophoresed and immunoblotted with an anti-ST2 IgM antibody (clone: G7). Duplicated samples after IP were treated with PNGaseF for 1 h and then immunoblotted simultaneously. Lane 1: anti-ST2-IP, lane 2: control antibody-IP, lane 3: control antibody-IP-PNGaseF-treated, lane 4: anti-ST2-IP-PNGaseF-treated. (**B**) Cell surface ST2L protein expression in LAD2 was analyzed with a FACS Calibur. FcR of LAD2 cells were blocked and then stained with an anti-ST2 antibody (2A5). FITC-goat anti-mouse IgG1 was used as the secondary antibody. Staining with control mouse IgG1 is shown with a black line and the anti-ST2 antibody is shown with the dotted red line.

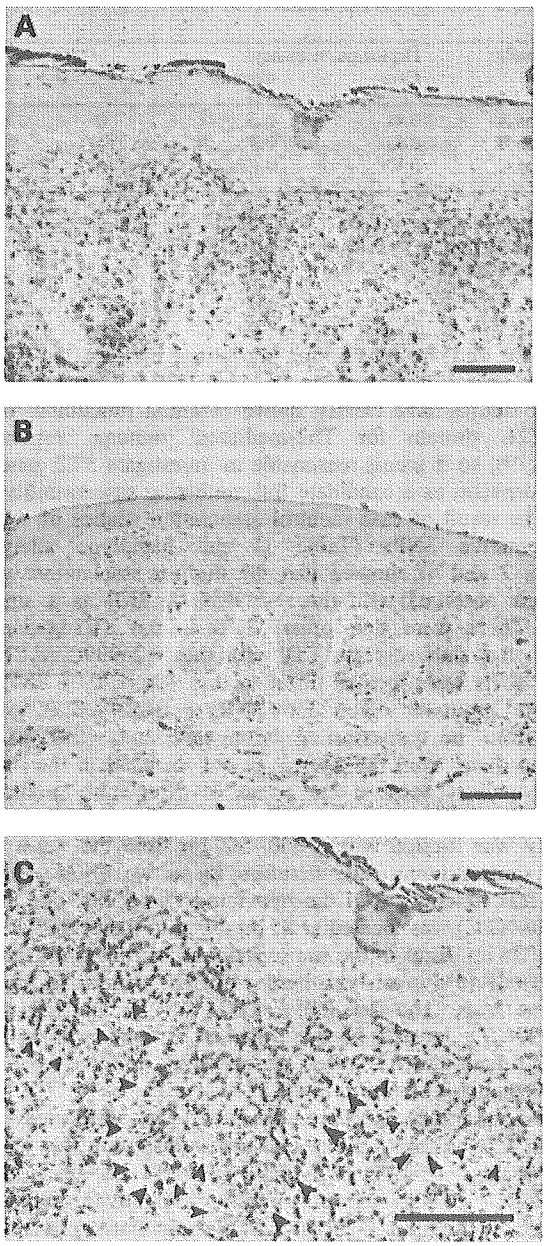

Figure 3. Immunohistochemical staining of human skin samples obtained from AD patients with anti-ST2 monoclonal antibody. Paraffin sections of AD skin biopsies were immunostained with an anti-ST2 antibody (HB12). (**A**) Skin biopsy from acute stage AD. Suprabasal layers of KC show membranous ST2-positive staining. Sporadic positive staining in the dermal region was also observed. (**B**) Skin biopsy from chronic stage AD. Some of the infiltrating cells in the dermal layer show positive ST2 staining. (**C**) High magnification of anti-ST2 immunostaining with acute stage AD. The arrowheads indicate the limit of basement membrane. Bar = 200 μm.

region predominantly affected hematopoietic cells. We found that both ST2L and sST2 mRNAs were expressed most abundantly in mast cells (Supplementary Material, Fig. S3) and confirmed ST2L expression on mast cells at the protein level by western blotting (Fig. 2A) and FACS analysis (Fig. 2B). Moritz *et al.* (14) reported that ST2L was selectively expressed during the development of mast cell lineage, and very recently Chen *et al.* (25) showed that ST2L could be one of the markers for mast cell progenitors in adult mice. These results suggested that abundant ST2L expression might positively affect the number of mature mast cells in the skin, as observed in the AD skin region

(26). The functional roles of ST2L in mast cells will be clarified with an ST2L overexpression system (10), and a study is ongoing.

The positive immunostaining around the cell membrane of suprabasal KC in the acute stage of AD (Fig. 3A and C) reflects the accumulated sST2 in intercellular space because ST2L mRNA expression in KC was not observed in experiments *in vitro*. This is consistent with a previous study that showed intense ST2 protein accumulation in mouse epidermis (27), and we think that serum extravasation during the acute stage of AD may induce sST2 expression in KC as observed in our *in vitro* study (Fig. 1C) (Supplementary Material, Fig. S3). On the other hand, a histological sample from the chronic phase of AD showed slight ST2 staining (Fig. 3B). This might be a reflection of the shift toward the Th1 dominant immunological character observed in the chronic stage of AD (1,28).

Another clinical feature of AD is a reduced skin innate immune response (1). ST2L expression could inhibit the TLR-dependent innate response by sequestering the adaptor molecules Myd88 and Mal (17). Several reports showed that both anti-ST2 antibodies and ST2-immunoglobulin fusion protein could abrogate the Th2 immune response and eosinophilic responses (18,29). Therefore, we consider that sST2/ST2L will be a good therapeutic target of AD and that understanding of the genetic predisposition for high ST2 promoter activity may contribute to the prevention of severe AD.

MATERIALS AND METHODS

Antibodies and cell lines

Anti-ST2 monoclonal antibodies (mouse IgG1; clones 2A5 and HB12) were purchased from MBL (Nagoya, Japan), and an anti-ST2 monoclonal antibody (mouse IgM; clone G7) was generated as previously described (30). Human mast cell line LAD2 was kindly provided by Dr Arnold Kirshenbaum (NIAID, NIH) and maintained as previously described (31). Human neonatal skin fibroblasts were obtained from RIKEN cell bank (Tsukuba, Japan), immortalized human normal keratinocyte cells (PHK16-06b) were obtained from the Japanese Collection of Research Bioresources (JCRB) cell bank (Osaka, Japan).

Subjects

All subjects with AD were diagnosed according to the criteria of Hanifin and Rajka (32). Peripheral blood was obtained from 452 AD patients (mean age 30.0, 11–64 years old at enrollment of the study; mean age 7.1, 0–45 years old at the onset of AD; 236 males and 216 females) from Takao Hospital, Shiga Medical College Hospital and Yokohama City University Hospital. Sera for sST2 ELISA assay were also obtained from some of the patients enrolled in this genetic study. As a control group, we analyzed 636 randomly selected population-based individuals (mean age 42.2, 18–70 years). We excluded the presence of asthma, AD and nasal allergy in the control population via careful interview by physicians. All individuals were Japanese and gave written informed consent to participate in the study (or, for individuals less than 16 years old, their parents gave consent), according to the rules of the process committee at SNP Research Center, RIKEN.

Screening for genetic polymorphisms

The ST2 genomic region targeted for SNP discovery included a 2.5 kb continuous region 5′ to exon 1a (distal promoter region) and a 2.5 kb continuous region 5′ to exon 1b (proximal promoter region) and 11 exons, each with a minimum of 200 bases of flanking intronic sequences (Fig. 1A). Primer sets (Supplementary Material, Table S1) were designed on the basis of the ST2 genomic sequence (GenBank accession no. AC007248). Each polymerase chain reaction (PCR) was carried out with 5 ng of genomic DNA from 24 individuals. Sequence reaction was performed with Big Dye Terminator v3.1 using an ABI 3700 DNA analyzer.

Genotyping

We genotyped a total of seven representative SNPs in the *ST2* gene selected on the basis of the allele frequency (MAF > 10%) and LD (Table 1) (Supplementary Material, Table S2 and Fig. S1). Additional typing was carried out for some SNPs, in relation to the functional assay for *ST2* genes. The SNP typing was carried out either with the invader assay (33) or with the Taqman genotyping assay using an ABI PRISM 7700 sequence detection system. Invader assay was performed with multiplex PCR products as the template. Taqman genotyping assay was carried out according to the manufacturer's protocol.

Statistical analysis

Allele frequencies in AD cases and controls were compared by the contingency χ^2-test. A *P*-value of less than 0.01, also in the case of multiple comparisons after Bonferroni adjustment, was considered to be statistically significant. ORs and 95% confidence intervals (95% CI) were calculated. Pairwise LD coefficients were calculated and expressed as r^2. Intragenic LD and haplotype analyses were performed using SNPAlyze v2.0 (DYNACOM, Chiba, Japan) as recommended by the manufacturer. We estimated haplotype frequencies using the expectation–maximization algorithm. Comparison in reporter gene assay was performed with Student's *t*-test. The association between the serum sST2 level or total IgE concentration and the genotype was evaluated by the Mann–Whitney *U*-test. A *P*-value of less than 0.05 was considered to be statistically significant.

Reporter gene assay

We subcloned 1131 bp distal promoter sequences continuous to exon 1a into pGL3 basic vector (Promega Corporation, Madison, WI, USA). Two SNPs in this region (−27084G/C and −26999G/A) were in the state of complete LD. We made two haplotype clones 1 (−27639A, −27084G, −26999G) and 2 (−27639G, −27084C, −26999A). Another set of constructs was made by deleting a 355 bp long promoter sequence

between two PstI sites, which contained the −27084G/C and −26999G/A SNPs as well as two putative GATA binding sequences (named distal-Δ355). All subcloned plasmids were verified by direct sequencing. We transfected the pGL3-ST2 promoter plasmid and pRL-TK renilla luciferase vector (Promega) as an internal control for transfection efficiency into human cell line LAD2 with DMRIE-C (Invitrogen, Carlsbad, CA, USA). After 24 h, luciferase activity was measured with a Dual Luciferase Reporter Assay Kit (Promega).

Measurement of sST2 protein and total IgE

The protein level of sST2 in the sera of AD patients was measured using human ST2 ELISA kits (MBL) following the manufacturer's protocol. The total IgE concentration in serum was measured by the FEIA method in a commercial laboratory.

RT–PCR analysis for differential promoter usage

mRNA was isolated from cultured cells (LAD2, KC and human dermal fibroblasts) with a Quick Prep micro-mRNA purification kit (Amersham Bioscience, Little Chalfont, UK). cDNA was made with the Super Script III First-Strand Synthesis System (Invitrogen) using oligo$(dT)_{20}$ primer. To distinguish promoter usage for specific cell types and subtypes (sST2/ST2L) of mRNA, we made sets of specific primers and performed RT–PCR as previously described (21).

IP and western blotting analysis

First, 1×10^7 LAD2 cells were solublized with lysis buffer [1% Triton X-100 in 20 mM Tris–HCl, pH 7.6, 150 mM NaCl with Complete Mini protease inhibitor cocktail tablets (Roche, Penzberg, Germany)]. The cell lysate was centrifuged at 20 000*g* for 15 min at 4°C. The supernatant was taken and pre-cleared with Protein-A Sepharose (Amersham) for 30 min. The sample was reacted with 2 μg of the anti-ST2 antibody (2A5) or control mouse IgG1 for 1 h and then Protein-A Sepharose was added. After 3 h rotation at 4°C, the Sepharose was washed with the lysis buffer and finally suspended with SDS sample buffer (50 mM Tris–HCl, pH 6.8, 2% SDS, 20% glycerol, 0.4% bromophenol blue, 50 mM DTT). To check the glycosylation status of ST2L protein, aliquots of the IP samples were treated with PNGaseF (New England Biolaboratory, Bevery, MA, USA). SDS–PAGE and subsequent immunoblotting were essentially performed as previously described (34). In brief, samples were subjected to SDS–PAGE using 4–20% Tris–glycine polyacrylamide gels and then electrophoretically transferred onto a PVDF membrane (Millipore). The membrane was incubated with the mouse anti-human ST2 IgM antibody (G7) overnight at 4°C. After washing with PBS, the membrane was reacted with a horseradish peroxidase (HRP)-conjugated anti-mouse IgM antibody for 30 min. The membrane was developed onto X-ray film with ECL plus (Amersham).

Flow cytometric analysis

Flow cytometric analysis was carried out using the anti-ST2 monoclonal antibody (2A5). LAD2 cells were washed with PBS, and Fc receptors (FcR) were blocked with FcR blocking reagent (Miltenyi Biotec, Gladbach, Germany). Cells were reacted with 4 μg of the anti-ST2 IgG monoclonal antibody in a volume of 40 μl for 15 min at room temperature. As a control, an isotype-matched mouse IgG1 antibody was used. After washing with PBS, the cells were reacted with an FITC-conjugated anti-mouse IgG antibody (Dako Japan, Kyoto). The stained cells were analyzed with a FACS Caliber (BD Japan).

Immunohistochemistry

ST2 immunohistochemistry was performed essentially as described previously (35). In brief, formaldehyde-fixed paraffin sections of the skin biopsies from AD patients were deparaffinized, then the endogenous peroxidase activity was quenched with 0.3% H_2O_2 in methanol for 20 min. Non-specific staining was blocked with blocking buffer (10% normal goat serum, 1% BSA in PBS) for 30 min. The anti-ST2 monoclonal antibody (clone HB12) was applied and reacted overnight at 4°C. After washing with PBS, slides were incubated with HRP-conjugated anti-mouse IgG for 30 min. The slides were developed with DAB (Dojindo, Kumamoto, Japan).

SUPPLEMENTARY MATERIAL

Supplementary Material is available at HMG Online.

ACKNOWLEDGEMENTS

We thank Dr Arnold Kirshenbaum for providing LAD2 cells, Professor Julian M. Hopkin for continuous supports and valuable comments, Miki Kokubo and Hiroshi Sekiguchi for their excellent technical assistance. This work was supported by a grant from the Japanese Millennium Project.

Conflict of Interest statement. None declared.

REFERENCES

1. Leung, D.Y., Boguniewicz, M., Howell, M.D., Nomura, I. and Hamid, Q.A. (2004) New insights into atopic dermatitis. *J. Clin. Invest.*, **113**, 651–657.
2. Lee, Y.A., Wahn, U., Kehrt, R., Tarani, L., Businco, L., Gustafsson, D., Andersson, F., Oranje, A.P., Wolkertstorfer, A., Von Berg, A. *et al.* (2000) A major susceptibility locus for atopic dermatitis maps to chromosome 3q21. *Nat. Genet.*, **26**, 470–473.
3. Bradley, M., Soderhall, C., Luthman, H., Wahlgren, C.F., Kockum, I. and Nordenskjold, M. (2002) Susceptibility loci for atopic dermatitis on chromosomes 3, 13, 15, 17 and 18 in a Swedish population. *Hum. Mol. Genet.*, **11**, 1539–1548.
4. Cookson, W.O., Ubhi, B., Lawrence, R., Abecasis, G.R., Walley, A.J., Cox, H.E., Coleman, R., Leaves, N.I., Trembath, R.C., Moffatt, M.F. *et al.* (2001) Genetic linkage of childhood atopic dermatitis to psoriasis susceptibility loci. *Nat. Genet.*, **27**, 372–373.
5. Schultz Larsen, F. (1993) Atopic dermatitis. A genetic-epidemiologic study in a population-based twin sample. *J. Am. Acad. Dermatol.*, **28**, 719–723.
6. Mao, X.Q., Kawai, M., Yamashita, T., Enomoto, T., Dake, Y., Sasaki, S., Kataoka, Y., Fukuzumi, T., Endo, K., Sano, H. *et al.* (2000) Imbalance production between interleukin-1beta (IL-1beta) and IL-1 receptor antagonist (IL-1Ra) in bronchial asthma. *Biochem. Biophys. Res. Commun.*, **276**, 607–612.

7. Karjalainen, J., Hulkkonen, J., Pessi, T., Huhtala, H., Nieminen, M.M., Aromaa, A., Klaukka, T. and Hurme, M. (2002) The IL1A genotype associates with atopy in nonasthmatic adults. *J. Allergy. Clin. Immunol.*, **110**, 429–434.
8. Wjst, M., Fischer, G., Immervoll, T., Jung, M., Saar, K., Rueschendorf, F., Reis, A., Ulbrecht, M., Gomolka, M., Weiss, E.H. *et al.* (1999) A genome-wide search for linkage to asthma. German Asthma Genetics Group. *Genomics*, **58**, 1–8.
9. Tominaga, S. (1989) A putative protein of a growth specific cDNA from BALB/c-3T3 cells is highly similar to the extracellular portion of mouse interleukin 1 receptor. *FEBS Lett.*, **258**, 301–304.
10. Li, H., Tago, K., Io, K., Kuroiwa, K., Arai, T., Iwahana, H., Tominaga, S. and Yanagisawa, K. (2000) The cloning and nucleotide sequence of human ST2L cDNA. *Genomics*, **67**, 284–290.
11. Tominaga, S., Kuroiwa, K., Tago, K., Iwahana, H., Yanagisawa, K. and Komatsu, N. (1999) Presence and expression of a novel variant form of *ST2* gene product in human leukemic cell line UT-7/GM. *Biochem. Biophys. Res. Commun.*, **264**, 14–18.
12. Yanagisawa, K., Naito, Y., Kuroiwa, K., Arai, T., Furukawa, Y., Tomizuka, H., Miura, Y., Kasahara, T., Tetsuka, T. and Tominaga, S. (1997) The expression of *ST2* gene in helper T cells and the binding of ST2 protein to myeloma-derived RPMI8226 cells. *J. Biochem. (Tokyo)*, **121**, 95–103.
13. Lohning, M., Stroehmann, A., Coyle, A.J., Grogan, J.L., Lin, S., Gutierrez-Ramos, J.C., Levinson, D., Radbruch, A. and Kamradt, T. (1998) T1/ST2 is preferentially expressed on murine Th2 cells, independent of interleukin 4, interleukin 5, and interleukin 10, and important for Th2 effector function. *Proc. Natl Acad. Sci. USA*, **95**, 6930–6935.
14. Moritz, D.R., Rodewald, H.R., Gheyselinck, J. and Klemenz, R. (1998) The IL-1 receptor-related T1 antigen is expressed on immature and mature mast cells and on fetal blood mast cell progenitors. *J. Immunol.*, **161**, 4866–4874.
15. Wollenberg, A. and Bieber, T. (2000) Atopic dermatitis: from the genes to skin lesions. *Allergy*, **55**, 205–213.
16. Trajkovic, V., Sweet, M.J. and Xu, D. (2004) T1/ST2—an IL-1 receptor-like modulator of immune responses. *Cytokine Growth Factor Rev.*, **15**, 87–95.
17. Brint, E.K., Xu, D., Liu, H., Dunne, A., McKenzie, A.N., O'Neill, L.A. and Liew, F.Y. (2004) ST2 is an inhibitor of interleukin 1 receptor and toll-like receptor 4 signaling and maintains endotoxin tolerance. *Nat. Immunol.*, **5**, 373–379.
18. Coyle, A.J., Lloyd, C., Tian, J., Nguyen, T., Erikkson, C., Wang, L., Ottoson, P., Persson, P., Delaney, T., Lehar, S. *et al.* (1999) Crucial role of the interleukin 1 receptor family member T1/ST2 in T helper cell type 2-mediated lung mucosal immune responses. *J. Exp. Med.*, **190**, 895–902.
19. Xu, D., Chan, W.L., Leung, B.P., Huang, F., Wheeler, R., Piedrafita, D., Robinson, J.H. and Liew, F.Y. (1998) Selective expression of a stable cell surface molecule on type 2 but not type 1 helper T cells. *J. Exp. Med.*, **187**, 787–794.
20. Hayakawa, M., Yanagisawa, K., Aoki, S., Hayakawa, H., Takezako, N. and Tominaga, S. (2005) T-helper type 2 cell-specific expression of the *ST2* gene is regulated by transcription factor GATA-3. *Biochim. Biophys. Acta*, **1728**, 53–64.
21. Iwahana, H., Yanagisawa, K., Ito-Kosaka, A., Kuroiwa, K., Tago, K., Komatsu, N., Katashima, R., Itakura, M. and Tominaga, S. (1999) Different promoter usage and multiple transcription initiation sites of the interleukin-1 receptor-related human *ST2* gene in UT-7 and TM12 cells. *Eur. J. Biochem.*, **264**, 397–406.
22. Halbert, A.R., Weston, W.L. and Morelli, J.G. (1995) Atopic dermatitis: is it an allergic disease? *J. Am. Acad. Dermatol.*, **33**, 1008–1018.
23. Untersmayr, E., Bakos, N., Scholl, I., Kundi, M., Roth-Walter, F., Szalai, K., Riemer, A.B., Ankersmit, H.J., Scheiner, O., Boltz-Nitulescu, G. *et al.* (2005) Anti-ulcer drugs promote IgE formation toward dietary antigens in adult patients. *FASEB J.*, **19**, 656–658.
24. Oshikawa, K., Kuroiwa, K., Tago, K., Iwahana, H., Yanagisawa, K., Ohno, S., Tominaga, S.I. and Sugiyama, Y. (2001) Elevated soluble ST2 protein levels in sera of patients with asthma with an acute exacerbation. *Am. J. Respir. Crit. Care Med.*, **164**, 277–281.
25. Chen, C.C., Grimbaldeston, M.A., Tsai, M., Weissman, I.L. and Galli, S.J. (2005) Identification of mast cell progenitors in adult mice. *Proc. Natl Acad. Sci. USA*, **102**, 11408–11413.
26. Damsgaard, T.E., Olesen, A.B., Sorensen, F.B., Thestrup-Pedersen, K. and Schiotz, P.O. (1997) Mast cells and atopic dermatitis. Stereological quantification of mast cells in atopic dermatitis and normal human skin. *Arch. Dermatol. Res.*, **289**, 256–260.
27. Rossler, U., Thomassen, E., Hultner, L., Baier, S., Danescu, J. and Werenskiold, A.K. (1995) Secreted and membrane-bound isoforms of T1, an orphan receptor related to IL-1-binding proteins, are differently expressed *in vivo*. *Dev. Biol.*, **168**, 86–97.
28. Grewe, M., Bruijnzeel-Koomen, C.A., Schopf, E., Thepen, T., Langeveld-Wildschut, A.G., Ruzicka, T. and Krutmann, J. (1998) A role for Th1 and Th2 cells in the immunopathogenesis of atopic dermatitis. *Immunol. Today*, **19**, 359–361.
29. Walzl, G., Matthews, S., Kendall, S., Gutierrez-Ramos, J.C., Coyle, A.J., Openshaw, P.J. and Hussell, T. (2001) Inhibition of T1/ST2 during respiratory syncytial virus infection prevents T helper cell type 2 (Th2)- but not Th1-driven immunopathology. *J. Exp. Med.*, **193**, 785–792.
30. Yoshida, K., Arai, T., Yokota, T., Komatsu, N., Miura, Y., Yanagisawa, K., Tetsuka, T. and Tominaga, S. (1995) Studies on natural *ST2* gene products in the human leukemic cell line UT-7 using monoclonal antihuman ST2 antibodies. *Hybridoma*, **14**, 419–427.
31. Kirshenbaum, A.S., Akin, C., Wu, Y., Rottem, M., Goff, J.P., Beaven, M.A., Rao, V.K. and Metcalfe, D.D. (2003) Characterization of novel stem cell factor responsive human mast cell lines LAD 1 and 2 established from a patient with mast cell sarcoma/leukemia; activation following aggregation of FcepsilonRI or FcgammaRI. *Leuk. Res.*, **27**, 677–682.
32. Hanifin, J.M. and Rajka, R.G. (1980) Diagnostic features of atopic dermatitis. *Acta Derm. Venereol.*, **92** (suppl.), 44–47.
33. Ohnishi, Y., Tanaka, T., Ozaki, K., Yamada, R., Suzuki, H. and Nakamura, Y. (2001) A high-throughput SNP typing system for genome-wide association studies. *J. Hum. Genet.*, **46**, 471–477.
34. Matsuda, A., Tagawa, Y., Matsuda, H. and Nishihira, J. (1996) Identification and immunohistochemical localization of macrophage migration inhibitory factor in human cornea. *FEBS Lett.*, **385**, 225–228.
35. Tsuchiya, T., Ohshima, K., Karube, K., Yamaguchi, T., Suefuji, H., Hamasaki, M., Kawasaki, C., Suzumiya, J., Tomonaga, M. and Kikuchi, M. (2004) Th1, Th2, and activated T-cell marker and clinical prognosis in peripheral T-cell lymphoma, unspecified: comparison with AILD, ALCL, lymphoblastic lymphoma, and ATLL. *Blood*, **103**, 236–241.

Human Molecular Genetics, 2005, Vol. 14, No. 19 *2779–2786*
doi:10.1093/hmg/ddi311
Advance Access published on August 22, 2005

Coding SNP in tenascin-C Fn-III-D domain associates with adult asthma

Akira Matsuda[1,*], Tomomitsu Hirota[1], Mitsuteru Akahoshi[1], Makiko Shimizu[1], Mayumi Tamari[1], Akihiko Miyatake[3], Atsushi Takahashi[2], Kazuko Nakashima[1,4], Naomi Takahashi[1], Kazuhiko Obara[1], Noriko Yuyama[5], Satoru Doi[6], Yumiko Kamogawa[7], Tadao Enomoto[9], Koichi Ohshima[10], Tatsuhiko Tsunoda[2], Shoichiro Miyatake[7], Kimie Fujita[11], Moriaki Kusakabe[12], Kenji Izuhara[13], Yusuke Nakamura[8], Julian Hopkin[14] and Taro Shirakawa[1,4]

[1]Laboratory for Genetics of Allergic Diseases and [2]Laboratory for Medical Informatics, SNP Research Center, RIKEN, Yokohama, Japan, [3]Miyatake Asthma Clinic, Osaka, Japan, [4]Department of Health Promotion and Human Behavior, Kyoto University Graduate School of Public Health, Kyoto, Japan, [5]Genox Research Inc., Kawasaki, Japan, [6]Osaka Prefectural Habikino Hospital, Osaka, Japan, [7]Department of Molecular and Developmental Biology and [8]Laboratory of Molecular Medicine, Human Genome Center, Institute of Medical Science, University of Tokyo, Tokyo, Japan, [9]Department of Otolaryngology, Japanese Red Cross Society, Wakayama Medical Center, Wakayama, Japan, [10]Department of Pathology, School of Medicine, Fukuoka University, Fukuoka, Japan, [11]College of Nursing, University of Shiga, Shiga, Japan, [12]Experimental Animal Research Center, Institute for Animal Reproduction, Ibaraki, Japan, [13]Department of Biomolecular Sciences, Saga Medical School, Saga, Japan and [14]Experimental Medicine Unit, University of Wales Swansea, Swansea, UK

Received June 20, 2005; Revised and Accepted August 9, 2005

The extracellular matrix glycoprotein tenascin-C (TNC) has been accepted as a valuable histopathological subepithelial marker for evaluating the severity of asthmatic disease and the therapeutic response to drugs. We found an association between an adult asthma and an SNP encoding TNC fibronectin type III-D (Fn-III-D) domain in a case–control study between a Japanese population including 446 adult asthmatic patients and 658 normal healthy controls. The SNP (44513A/T in exon 17) strongly associates with adult bronchial asthma (χ^2 test, $P = 0.00019$, Odds ratio = 1.76, 95% confidence interval = 1.31–2.36). This coding SNP induces an amino acid substitution (Leu1677Ile) within the Fn-III-D domain of the alternative splicing region. Computer-assisted protein structure modeling suggests that the substituted amino acid locates at the outer edge of the beta-sheet in Fn-III-D domain and causes instability of this beta-sheet. As the TNC fibronectin-III domain has molecular elasticity, the structural change may affect the integrity and stiffness of asthmatic airways. In addition, TNC expression in lung fibroblasts increases with Th2 immune cytokine stimulation. Thus, Leu1677Ile may be valuable marker for evaluating the risk for developing asthma and plays a role in its pathogenesis.

INTRODUCTION

Asthma is a chronic inflammatory disease characterized by smooth muscle hypertrophy, excess mucus secretion and increased deposition of extracellular matrix (ECM) around the basement membrane (1–3). Many asthmatic patients also have an atopic tendency characterized by a Th2 dominant cytokine profile including interleukin (IL)-4 and IL-13 (4). Several studies showed genetic associations between asthma and proteinases like ADAM33 (5) or Th2 cytokine receptors (4,6), but to the best of our knowledge, there is no report of an association between asthma and ECM genes. The hexametric

*To whom correspondence should be addressed at: Laboratory for Genetics of Allergic Diseases, SNP Research Center, RIKEN, Suehiro 1-7-22, Tsurumi-KU, Yokohama 230-0045, Japan. Tel: +81 455039616; Fax: +81 455039615; Email: akimatsu@src.riken.go.jp

ECM glycoprotein tenascin-C (TNC) has been accepted as a histopathological marker, beneath the asthmatic airway, for evaluating the severity and the therapeutic effects of drugs in bronchial asthma (7,8) because of its tightly controlled expression pattern. TNC expression is prominently increased around airway basement membranes of asthmatic patients (8), and two independent microarray experiments, including our own, identified TNC as one of the IL-4- or IL-13-induced genes in human bronchial epithelial cells (9,10). Recent studies showed that the fibronectin-III (Fn-III) domain of TNC has molecular elasticity (11) and mechanical strain can induce TNC expression (12), so we consider TNC to be more than just a marker for asthmatic pathology.

In the present study, we show the genetic association between an adult asthma and an SNP in exon 17 (44513A/T) causing amino acid substitution in the fibronectin type III-D (Fn-III-D) domain region of TNC gene (13). We carried out protein structure modeling of the Fn-III-D domain and found that the amino acid replacement Leu1677Ile could affect the structural stability of the Fn-III-D domain, which might affect the elasticity of the domain. In addition, TNC expression in lung fibroblasts was increased with IL-4 or IL-13 stimulation. The aim of our study was to test the association between the coding SNP in the TNC Fn-III-D domain and asthma and to determine how the SNP may affect the pathophysiology of asthma.

RESULTS

Identification of TNC genetic polymorphisms and selection of representative SNPs

We detected 62 genetic polymorphisms within the TNC region (Supplementary Material, Table S1) by resequencing samples from 24 Japanese individuals (12 asthmatics and 12 controls). Of these, we selected 23 SNPs whose minor allele frequency (MAF) was >20%. To check the intragenic linkage disequilibrium (LD) pattern in the TNC gene, pairwise LD was measured by r among the 23 SNPs (Fig. 1A). We selected 10 representative SNPs on the basis of location and LD with other sites; the positions of the 10 SNPs are shown in Figure 1B.

Case–control association study using asthmatic patients

We carried out a case–control association study using a Japanese asthmatic population. Clinical characteristics of the bronchial asthma patients are presented in Table 1. The severity of asthma before treatment was classified by the Global Initiative for Asthma Guideline (14). All 10 investigated SNPs were within the Hardy–Weinberg equilibrium. The overall success rate for genotyping was 99.1%. Of these 10, an SNP in exon 17 (44513A/T) had a significant association with adult bronchial asthma in our Japanese cohort under a recessive model [χ^2 test, 44513TT versus AT + AA, raw P-value 0.00019, Odds ratio (OR) 1.76, 95% confidence interval (95% CI) = 1.31–2.36] (Table 2). Stronger association was observed when we limited case subjects to non-smoking asthmatics (44513TT versus AT + AA, raw P-value 0.000025, OR 2.06, 95% CI = 1.45–2.87). There was no correlation between the severity of asthma and the TNC genetic association (data not shown).

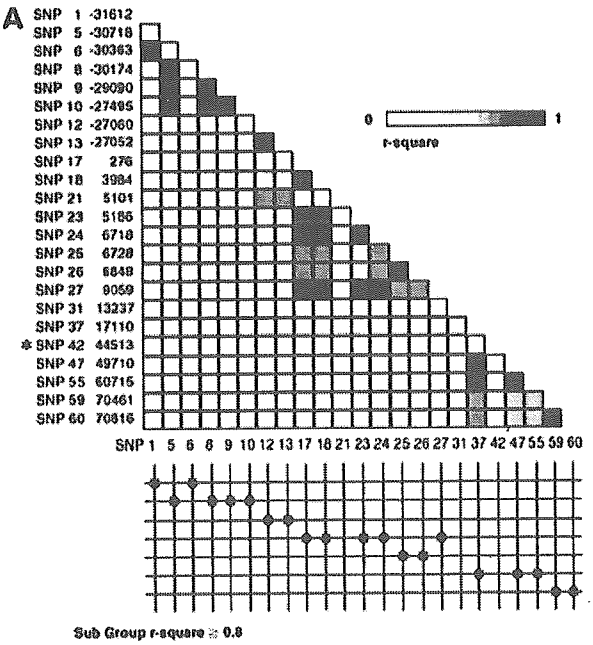

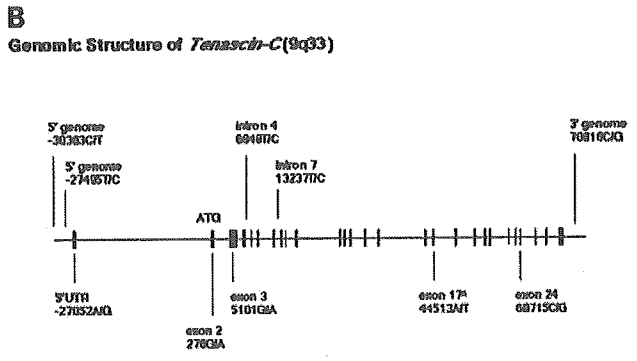

Figure 1. Pairwise LD map and SNP map in the TNC genomic region. (**A**) Pairwise LD in the TNC gene, as measured by the r^2 value between all pairs of SNPs examined. The position of 44513A/T is indicated with an asterisk and the remaining nine SNPs genotyped were indicated with red color. (**B**) The complete coding region of TNC, intron/exon boundaries, the intronic sequence, ~3 kb of 5′ genomic DNA and 1 kb of 3′ genomic DNA are shown. Twenty-seven exons are indicated by closed squares. Position 1 is the start codon of the TNC gene. An asterisk indicates the 44513A/T SNP.

LD mapping around the TNC gene

To exclude the possibility that our results reflected the association of other genes near the TNC locus with asthma, we constructed an LD map around the TNC gene locus using 48 SNPs (MAF > 10%). The results indicated that 44513A/T (indicated by an asterisk in Fig. 2) was located in the LD block extended from intron 8 of the TNC gene to the 3′ genome region of TNC (30 kb upstream and 20 kb downstream of this SNP) and that there were no other genes in this block (Fig. 2).

Table 1. Clinical characteristics of the bronchial asthma patients

Pretreatment: severity of disease[a]	Frequency of attack before treatment	Mean age	Mean age at onset	Mean duration of asthma (years)
Class 1: intermittent	Less than once a week	31.1	14.4	14.0
Class 2: mild persistent	More than once a week, less than once a day	45.9	30.6	16.0
Class 3: moderate persistent	Symptoms daily	47.1	36.5	19.8
Class 4: severe persistent	Symptoms daily, frequent nocturnal asthma	54.2	40.7	15.2

[a]Severity of disease was classified by Global Initiative for Asthma Guideline (14).

Table 2. Genotype frequencies for TNC SNPs and asthma susceptibility

SNP location	Control ($n = 658$) (%)			Bronchial asthma ($n = 446$) (%)			*P*-value[a]	*P*-value[b]	*P*-value[c]
	1	2	3	1	2	3			
−30363C/T	464 (71)	178 (27)	16 (2)	313 (71)	124 (29)	5 (0)	NS	NS	NS
−27495T/C	268 (41)	306 (47)	79 (12)	182 (41)	205 (47)	55 (12)	NS	NS	NS
−27052A/G	254 (39)	318 (49)	79 (12)	171 (39)	207 (47)	64 (14)	NS	NS	NS
276G/A	302 (46)	275 (42)	73 (11)	213 (48)	191 (43)	37 (9)	NS	NS	NS
5101G/A	301 (46)	299 (46)	56 (9)	197 (44)	200 (45)	49 (12)	NS	NS	NS
6848T/C	212 (32)	323 (49)	118 (18)	164 (37)	203 (46)	75 (17)	NS	NS	NS
13237T/C	340 (52)	269 (41)	46 (7)	229 (52)	180 (41)	29 (7)	NS	NS	NS
44513A/T	169 (26)	303 (46)	183 (28)	125 (29)	233 (53)	79 (18)	0.037	NS	0.0019
60715C/G	237 (36)	301 (46)	116 (18)	134 (30)	218 (49)	90 (20)	NS	NS	NS
70816C/G	279 (43)	284 (44)	87 (13)	178 (41)	193 (45)	61 (14)	NS	NS	NS

P-value adjusted with Bonferroni correction (raw *P*-values were multiplied by 10); NS, not significant.
[a]Allelel versus allele 2.
[b]Genotypell versus genotype 12 + 22.
[c]Genotype11 + 12 versus genotype 22.

Haplotype analysis

We carried out haplotype analysis of four representative SNPs in the LD block containing the 44513A/T SNP. Estimated frequencies of the four-locus haplotype were compared between cases and control subjects. The results of association studies for each haplotype showed a significant association between haplotype 1 and asthma (Table 3) (raw *P*-value = 0.004); however, the association was not stronger than that observed for the single locus (44513A/T).

Immunohistochemistry of TNC

Paraffin sections of asthmatic lungs were immunostained with a rat anti-TNC monoclonal antibody. Subepithelial deposition of TNC protein was observed beneath the bronchial epithelium in the asthmatic lung of a 65-year-old male (Fig. 3A). No apparent TNC staining was observed in the control lung of a 68-year-old male (Fig. 3B).

Computer modeling of the TNC Fn-III-D domain structure

We derived a protein structure model of the TNC Fn-III-D domain with MOE software (Fig. 4) to examine the possible effects of the substitution of the 1677th amino acid. The major allele in the normal population 44513-T encodes 1677Leu, whereas 44513-A, common in asthmatic patients, encodes 1677Ile. The 1677th amino acid is located at the beta-strand, which makes up the outermost side of the beta-sheet (Fig. 4A and B). The amino acid faces to the inside of the beta-sheet structure and there is a hydrophobic interaction between Phe1636, Leu1638, Leu1652, Ile1654 and Leu1680 (Fig. 4C, shaded region). The substitution of Leu1677Ile could result in steric hindrance with Phe1636 because of its side chain (Fig. 4D).

Identification of TNC variant expression in normal human lung fibroblasts by RT–PCR and western blotting

To confirm the expression of the TNC mRNA variant containing SNP 44513A/T in exon 17, RT–PCR (reverse transcription–polymerase chain reaction) was performed with a forward primer in exon 10 and a reverse primer in exon 19. The PCR results showed bands of 1969, 607 and 331 bp with normal human lung fibroblasts (NHLF) cDNA (Fig. 5A, left). The PCR products were subcloned and then sequenced. Larger bands (1969 and 607 bp) contained the Fn-III-D domain, including SNP 44513A/T. The cell lysate of NHLF was electrophoresed and immunoblotted with the rat anti-TNC antibody. A 250 kDa variant of TNC, corresponding to the largest mRNA, was dominantly expressed in NHLF, and both IL-4 and IL-13 could upregulate the 250 kDa TNC protein expression (Fig. 5B).

DISCUSSION

In the present study, asthmatic patients were recruited on the basis of the clinical asthma findings (14). We selected well-controlled cases after asthma treatments, (for class 2, 3 and

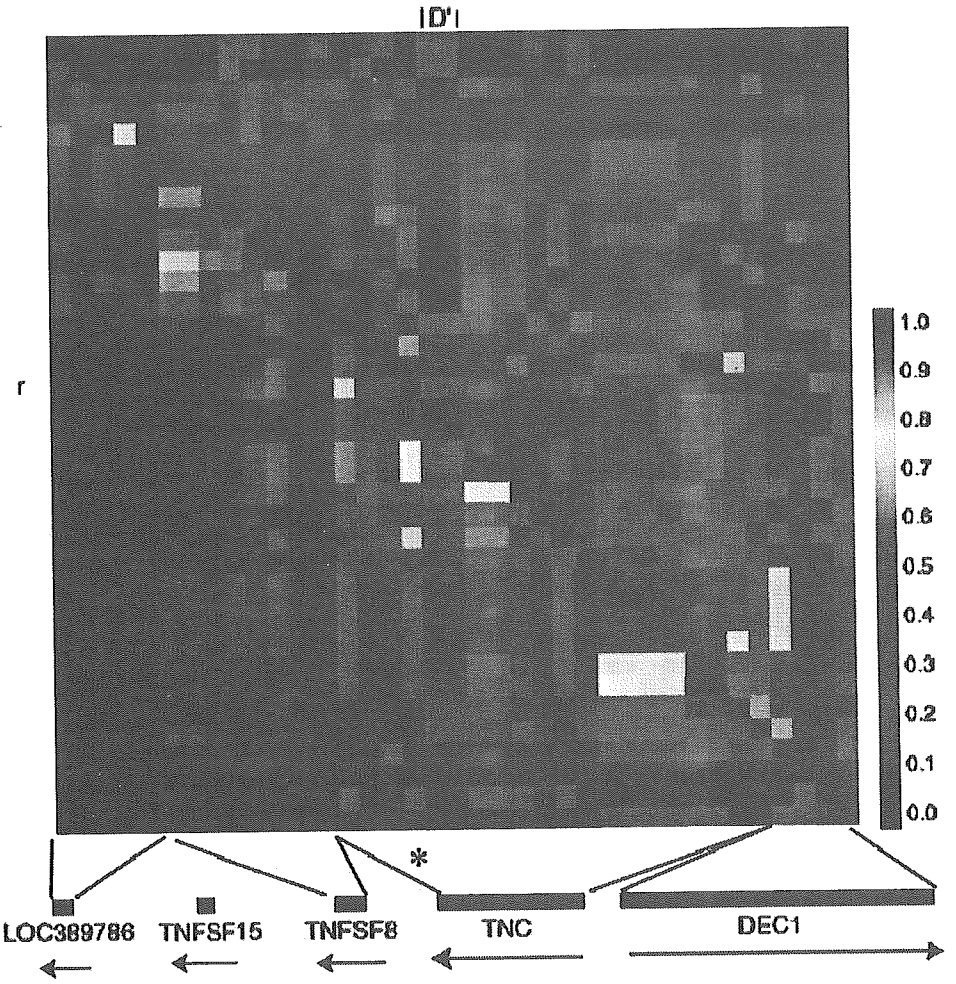

Figure 2. Pairwise LD map around TNC locus, as measured by D' value or r value. Pairwise LD map around the TNC locus, as measured by D' value or r value between all pairs of SNPs examined. The position of 44513A/T is indicated with an asterisk. Arrows indicate the direction of transcription of the genes.

4 cases with known amounts of an inhaled steroid: beclomethasone dipropionate; BDP), to ensure the reversibility of lung functions (Table 1). We took care to exclude possible COPD (chronic obstructive pulmonary disease) cases by spirometric analysis to check the reversibility of airflow obstruction and by X-ray/CT examinations. We found a genetic association between SNP 44513A/T in exon 17, coding the 1677th amino acid in the Fn-III-D domain, and adult bronchial asthma (Table 2). The genetic association between 44513A/T and asthma became stronger when we limited the analysis to the non-smoker asthmatic subpopulation. This result suggested that the association was not the consequence of secondary impairment of lung function due to smoking. The LD map around the TNC gene region showed that SNP 44513A/T was located in the LD block that extended from intron 8 to the 3′ genomic region of the TNC gene, and there were no other genes in the block (Fig. 2). Therefore, we concluded that the strong association observed with the SNP 44513A/T originated from the TNC gene itself. We intensively searched SNPs around the 44513A/T by resequencing and using public SNP databases, but we could not find any SNPs showing tight LD with 44513A/T. Weak LD was observed with 60715C/G (a coding SNP in exon 24) but there was no association between that SNP and bronchial asthma (Table 2), and the association between the four-SNP haplotypes including these two SNPs and asthma was not stronger than that of the 44513A/T single locus (Table. 3). Therefore, we selected SNP 44513A/T as the target for further analysis.

The TNC gene was chosen as a candidate gene for asthma on the basis of our previous GeneChip experiment (9). According to the results, TNC was one of the few genes constantly upregulated in bronchial epithelial cells in response to Th2 cytokines. We analyzed several candidate genes on the basis of the GeneChip results and found a significant

Table 3. Haplotype structure and frequency in TNC

Haplotype	SNP position				Haplotype frequency		*P*-value[a]	OR
	13237T/C	44513A/T	60715C/G	70816C/G	Controls	Cases		
Haplotype 1	T	T	C	C	0.33	0.27	0.004	1.33
Haplotype 2	T	A	G	G	0.26	0.27	0.725	1.04
Haplotype 3	C	T	C	C	0.17	0.17	0.816	1.03
Haplotype 4	C	A	G	G	0.08	0.08	0.933	1.01

OR, odds ratio.
[a]Analysis using a 2×2 table for each haplotype against all others combined in cases and controls.

association with the TNC gene. Furthermore, one previous genome-wide linkage study by Wjst *et al.* (15) showed that D9S1784 and D9S195 markers at chromosome 9q33 could be linked to asthma. TNC genes were located between these two markers (~9.7 Mb to D9S1784 and 5 Mb to D9S195). On the basis of these results, TNC seemed to be a good candidate gene for affecting susceptibility to asthma.

Our immunohistochemical staining of asthmatic airways showed TNC deposition around the basement membrane (Fig. 3A). Both bronchial epithelial cells and lung fibroblasts under the basement membrane may produce TNC. *In situ* hybridization experiments with the developing human lung (16) and respiratory distress syndrome (17) have shown that myofibroblasts under the epithelium express TNC mRNA. Therefore, we suppose that TNC in the asthmatic lung is predominantly produced by lung fibroblasts. It should be noted that the TNC Fn-III domain has both molecular elasticity (11) and essential roles for airway branching (18,19). We considered that TNC around the airway might have homeostatic roles for maintaining the integrity of airways in stressed conditions like bronchial asthma.

The structural model of the TNC Fn-III-D domain showed that the Ile1677 variant caused instability of the beta-sheet in the domain (Fig. 4D). Thus, Ile1677, a common variant among adult asthmatic patients, may alter the molecular elasticity of the TNC Fn-III domain. Airway resistance measurements of the asthmatic patients with or without allele 44513-A to investigate genotype–phenotype association are now ongoing.

It is known that a part of the TNC Fn-III domain, Fn-III-A1 through Fn-III-D, (Fig. 5A), is alternatively spliced (13). We checked the alternative splicing exon–intron junction for SNPs that might affect the splicing sites (20), but we could not find any SNPs that showed a significant association with asthma. Previous reports showed that the large form of TNC, including the alternative splicing region, was the predominant form in developing rat lung (19). Thus, it is likely that the large form of TNC is the main variant in the lung. Our monoclonal antibody could not distinguish between the large and small forms of TNC in immunohistochemistry, so we further analyzed the TNC variants by RT–PCR and by western blotting using NHLF. We showed that 250 and 190 kDa TNC variants contained the alternatively spliced Fn-III-D domain in NHLF (Fig. 5A) and either IL-4 or IL-13 treatment could preferentially induce the 250 kDa variant (Fig. 5B). We also found that the induction of TNC mRNA by IL-4 and IL-13 was not the consequence of non-specific inflammation because STAT6 activation could upregulate TNC mRNA expression (Supplementary Material, Fig. S3). From these findings, we conclude that it is highly likely that SNP 44513A/T in the TNC Fn-III-D domain is functional, especially under the influence of Th2 cytokines.

There are a few studies analyzing the role of TNC in pathologic conditions, some of which showed homeostatic roles of TNC protein (21,22). Habu snake-venom toxin induces glomerulonephritis phenotype in TNC knockout mice with more severe disease than that in congenic control mice (23). We suppose that TNC is a molecule with homeostatic functions emergent under stressful conditions. The TNC molecule may also have homeostatic roles in asthmatic conditions and the instability of the Fn-III-D structure caused by this SNP may hence affect the pathophysiology of asthma.

In conclusion, we found a genetic association between the SNP encoding the Fn-III-D domain of the TNC molecule and the adult bronchial asthma. The coding SNP causes instability of the Fn-III-D domain structure. Under the influences of Th2 cytokines, the expression and functional impact of the TNC molecule increase. The coding SNP might be a useful marker for evaluating the risk for adult asthma and provides insights into the precise functional roles of TNC in the pathogenesis of asthma. Further study is needed.

MATERIALS AND METHODS

Materials

The rat anti-human TNC monoclonal antibody (clone 3–6) was described previously (24). A horseradish peroxidase (HRP)-conjugated goat anti-rat IgG antibody and precast Tris–glycine polyacrylamide gels were purchased from Invitrogen (Carlsbad, CA, USA). Recombinant human IL-4 and IL-13 were purchased from Peprotec (London, UK).

Cell culture

NHLF were purchased from BioWhittaker (Walkersville, MD, USA) and cultured with the fibroblast basal medium from the same company according to the manufacturer's protocol.

Subjects

The adult asthmatic patients were recruited from approximately 4000 outpatients who were diagnosed as having bronchial asthma at the Miyatake Asthma Clinic or at the Osaka Prefectural Habikino Hospital by asthma specialists using

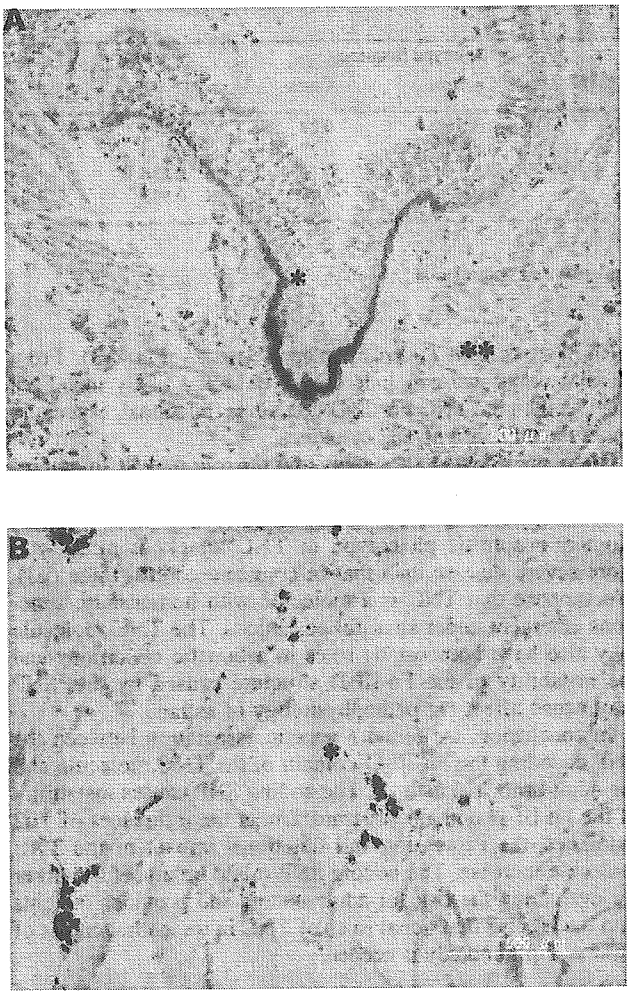

Figure 3. Immunohistochemical analysis of asthmatic lung with TNC antibody. Paraffin sections of asthmatic and control lungs were immunostained with the anti-TNC monoclonal antibody and visualized with indirect immunoperoxidase staining. Intense subepithelial staining is observed in the asthmatic lung (**A**) but not in the control lung (**B**) * indicates bronchial epithelium and ** indicates airway smooth muscle. Dark black spots in the control lung are foreign particles in the lung.

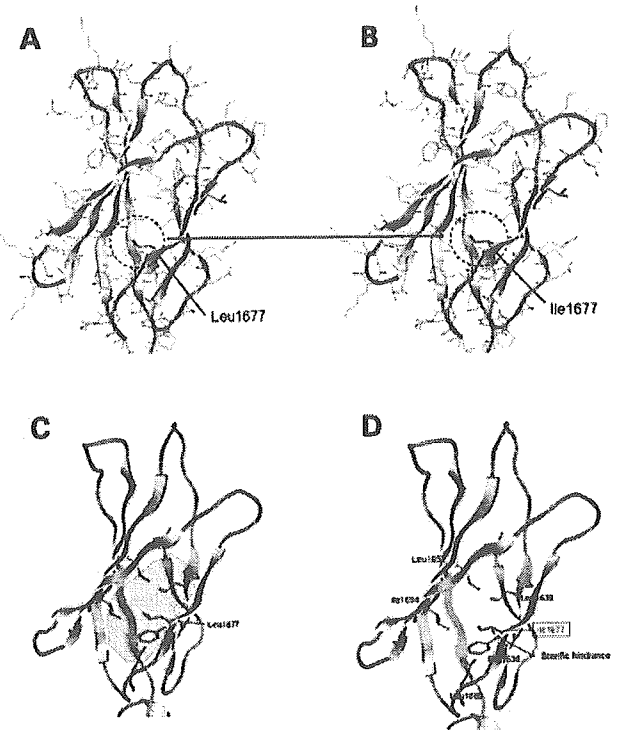

Figure 4. Computer modeling of TNC Fn-III-D domain and effect of 1677 Leu-Ile substitution. The 2.25 Åcrystal structure of chicken TNC (PDB accession no. P24821) was used as a template for homology modeling of the human TNC Fn-III-D domain. (**A**) The amino acid Leu1667 located in the fifth beta-sheet (yellow arrow, downward, indicated by black arrow) of the TNC Fn-III-D domain is shown with a green bar. (**B**) Amino acid Ile1677 located in the fifth beta-sheet of the TNC Fn-III-D domain is shown with a red bar. (**C**) Leu1677 makes a hydrophobic interaction plane (shaded region) among the hydrophobic amino acids. (**D**) The change of the amino acid from Leu to Ile caused steric hindrance with Phe1636 inside the beta-sheet.

the American Thoracic Society criteria as previously described (25,26). We selected 446 adult bronchial asthma patients (mean age 46.9, 16–70 years; male:female ratio, 1.0:1.2; mean serum IgE level, 741.3 U/ml; mite RAST positive 64.9%) satisfying the following symptoms and physical examination criteria: (i) those who showed episodic breathlessness, wheezing and chest tightness before treatment, (ii) the asthmatic symptoms were well controlled with known amounts of inhaled steroids. Among them, 105 patients were smokers or ex-smokers but not heavy smokers judged by the Fagerstrom Tolerance Questionnaire (26). Detailed information about the patients, including the severity of asthma (14) is summarized in Table 1. Peak expiratory flow analysis, spirometry, chest X-ray and CT scan were performed for the patients in need of differential diagnosis for COPD. Bronchial hyper-responsiveness was not tested. Peripheral blood was obtained from these 505 adult bronchial asthma patients. As a healthy control group, we analyzed 625 randomly selected population-based individuals (mean age 42.0, 18–69 years; male:female ratio, 2.5:1.0). We excluded the presence of asthma, atopic dermatitis and nasal allergies in the control population through careful interviews by physicians. All individuals were of Japanese origin and gave written informed consent to participate in the study, according to the process committee at SNP Research Center, RIKEN.

SNP discovery and genotyping in TNC gene

The TNC region targeted for SNP discovery included a 5 kb continuous region 5′ to the gene and 28 exons, each with a minimum 200 bp of a flanking intronic sequence. Forty primer sets were designed on the basis of TNC genomic sequences (Supplementary Material, Table S2). Each PCR was performed with 5 ng of genomic DNA from 24 individuals (12 asthmatic patients and 12 controls). The PCR product was reacted with BigDye Terminator v3.1 (Applied

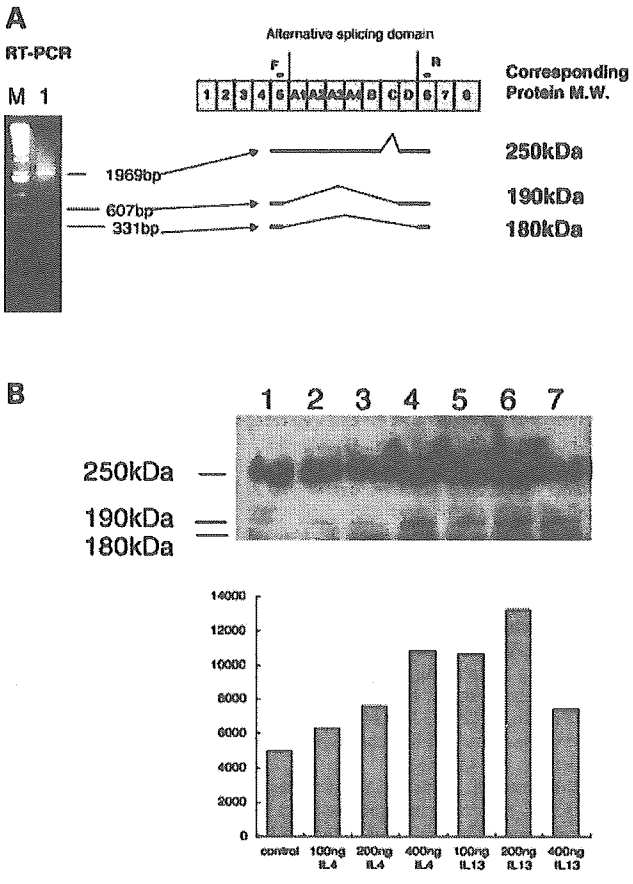

Figure 5. RT–PCR and western blot analysis for TNC variants in NHLF with Th2 cytokine stimulation. (**A**) TNC mRNA expression in NHLF was examined with RT–PCR. Subconfluent NHLF were stimulated with 100 ng/ml IL-13 for 72 h. After mRNA extraction and cDNA synthesis, PCR was performed with a pair of primers designed to differentiate alternatively spliced mRNA of TNC. The PCR products were electrophoresed on 1% agarose gel. M: 1 kb DNA marker and Lane 1: NHLF (left side). The structure of the FN-III domain in the human TNC gene is shown (center). F: forward primer and R: reverse primer. Corresponding protein molecular weights (M.W.) are indicated to the right. (**B**) Western blot analysis of NHLF culture samples stimulated with IL-4 or with IL-13 for 72 h. The samples were electrophoresed in 4–20% Tris–glycine gels and electrotransferred in PVDF membrane. Immunoblotting was performed with the rat anti-TNC monoclonal antibody. The relative intensity of TNC protein was quantified with NIH Image and is shown at the bottom. Lane 1 represents NHLF without stimulation. Lanes 2–4 represent NHLF stimulated with IL-4 at the concentrations of 100, 200 and 400 ng/ml, respectively. Lanes 5–7 represent NHLF stimulated with IL-13 at the concentrations of 100, 200 and 400 ng/ml, respectively.

Biosystems). We also utilized the SNP information from the database of SNPs by Japanese Science and Technology Agency database (JSNP). Intragenic pairwise LD in the TNC locus was examined by measuring r^2 among 22 SNPs. The pairwise LD and haplotype were evaluated using the SNPAlyze 3.1 software (Dynacom Co. Ltd, Chiba, Japan). Position SNPs were numbered according to their position relative to the published genomic sequence containing the TNC region (GenBank accession no. AL162425), and position 1 is the adenine of the first methionine of TNC. The panel of 10 SNPs was genotyped with the multiplex PCR-Invader assay or Taqman genotyping system as described previously (27). To investigate the pattern of LD in and around the TNC locus, pairwise LD coefficients were calculated and expressed as $|D'|$ or r. We evaluated the LD extension of the TNC genomic region with 48 SNPs registered in JSNP by genotyping 1041 general Japanese subjects.

Statistical analysis

Allele frequencies in bronchial asthma and controls were compared by the contingency χ^2 test. A P-value of less than 0.01, after Bonferroni adjustment in case of multiple comparisons, was considered to be statistically significant. The OR and 95% CI were also calculated. Haplotype frequencies were estimated by the expectation-maximization algorithm.

TNC immunohistochemistry

TNC immunohistochemistry was performed essentially as previously described (24). Fresh human lung tissues were obtained and embedded in paraffin from patients undergoing surgery; informed consent was obtained. Asthmatic lung specimen was obtained from autopsied lung. The sections were deparaffined and endogenous peroxidase activity was quenched with 0.3% H_2O_2 in methanol for 20 min. Non-specific staining was blocked with blocking buffer [10% normal goat serum and 1% bovine serum albumin in phosphate-buffered saline (PBS)] for 30 min. The rat anti-human TNC antibody (10 μg/ml) was applied and reacted overnight at 4°C. After PBS washing, slides were incubated with HRP-conjugated anti-rat IgG antibody for 30 min. The slides were developed with DAB (Dojindo, Kumamoto, Japan) in Tris-buffered saline with 0.05% H_2O_2.

Computer modeling of TNC Fn-III-D protein structure

To examine the effect of amino acid substitution at position 1677 in the Fn-III-D domain, protein structural modeling was performed using MOE software (Chemical Computing Group Inc., Montreal, Canada). The coordinates of the 2.25 Å crystal structure of the chicken TNC Fn-III domain (PDB accession no. P24821) were used as a template for homology modeling of the human TNC Fn-III-D domain. The two structures were further minimized with AMBER 94 using MOE software. Both Leu1677 Ile variants of the TNC Fn-III-D domain were built up using the same program.

RT–PCR and western blotting analysis for TNC variants detection

Subconfluent NHLF were stimulated with 100 ng/ml IL-13 for 72 h and mRNA was isolated using a QuickPrep micro mRNA purification kit (Amersham, Uppsala, Sweden). cDNA was made with the SuperScript III First-Strand Synthesis System (Invitrogen, Carlsbad, CA, USA) using oligo$(dT)_{20}$ primer. RT–PCR was carried out for 5 min at 95°C for initial denaturing, followed by 35 cycles of 95°C for 60 s, 52°C for 60 s, and 72°C for 120 s, in the GeneAmp PCR System 9700 (Applied Biosystems). The primer TNC-3089: ACCGCTACCGCCT

CAATTACA and TNC-5331: GGTTCCGTCCACAGT TACCA were set to distinguish mRNA variants due to alternative splicing (13). The PCR products were electrophoresed in 1% agarose gel and distinct bands were excised. DNA was extracted from the excised bands with a DNA Gel Extraction Kit (Millipore, Tokyo, Japan) and subcloned into pCR II-TOPO cloning vector (Invitrogen). The subcloned inserts were read by sequencing. For western blotting, subconfluent NHLF were stimulated either with IL-4 or with IL-13 for 72 h at the concentration indicated in Fig. 5. The NHLF were solublized with SDS sample buffer (50 mM Tris–HCl pH6.8, 2% SDS, 20% glycerol, 0.4% bromophenol blue, 50 mM DTT). SDS–PAGE and subsequent immunoblotting were performed as previously described (21).

SUPPLEMENTARY MATERIAL

Supplementary Material is available at HMG Online.

ACKNOWLEDGEMENTS

We thank Professor M. Munakata for comments and suggestions, Miki Kokubo and Hiroshi Sekiguchi for their excellent technical assistance and members of The Rotary Club of Osaka-Midosuji District 2660 Rotary International in Japan for supporting our study. This work was supported by a grant from the Japanese Millennium Project.

Conflict of Interest statement. None declared.

REFERENCES

1. Callerame, M.L., Condemi, J.J., Bohrod, M.G. and Vaughan, J.H. (1971) Immunologic reactions of bronchial tissues in asthma. *N. Engl. J. Med.*, **284**, 459–464.
2. Carroll, N., Elliot, J., Morton, A. and James, A. (1993) The structure of large and small airways in nonfatal and fatal asthma. *Am. Rev. Respir. Dis.*, **147**, 405–410.
3. Cohn, L., Elias, J.A. and Chupp, G.L. (2004) Asthma: mechanisms of disease persistence and progression. *Annu. Rev. Immunol.*, **22**, 789–815.
4. Heinzmann, A., Mao, X.Q., Akaiwa, M., Kreomer, R.T., Gao, P.S., Ohshima, K., Umeshita, R., Abe, Y., Braun, S., Yamashita, T. *et al.* (2000) Genetic variants of IL-13 signalling and human asthma and atopy. *Hum. Mol. Genet.*, **9**, 549–559.
5. Van Eerdewegh, P., Little, R.D., Dupuis, J., Del Mastro, R.G., Falls, K., Simon, J., Torrey, D., Pandit, S., McKenny, J., Braunschweiger, K. *et al.* (2002) Association of the *ADAM33* gene with asthma and bronchial hyperresponsiveness. *Nature*, **418**, 426–430.
6. Mitsuyasu, H., Izuhara, K., Mao, X.Q., Gao, P.S., Arinobu, Y., Enomoto, T., Kawai, M., Sasaki, S., Dake, Y., Hamasaki, N. *et al.* (1998) Ile50Val variant of IL4R alpha upregulates IgE synthesis and associates with atopic asthma. *Nat. Genet.*, **19**, 119–120.
7. Flood-Page, P., Menzies-Gow, A., Phipps, S., Ying, S., Wangoo, A., Ludwig, M.S., Barnes, N., Robinson, D. and Kay, A.B. (2003) Anti-IL-5 treatment reduces deposition of ECM proteins in the bronchial subepithelial basement membrane of mild atopic asthmatics. *J. Clin. Invest.*, **112**, 1029–1036.
8. Laitinen, A., Altraja, A., Kampe, M., Linden, M., Virtanen, I. and Laitinen, L.A. (1997) Tenascin is increased in airway basement membrane of asthmatics and decreased by an inhaled steroid. *Am. J. Respir. Crit. Care Med.*, **156**, 951–958.
9. Yuyama, N., Davies, D.E., Akaiwa, M., Matsui, K., Hamasaki, Y., Suminami, Y., Yoshida, N.L., Maeda, M., Pandit, A., Lordan, J.L. *et al.* (2002) Analysis of novel disease-related genes in bronchial asthma. *Cytokine*, **19**, 287–296.
10. Lee, J.H., Kaminski, N., Dolganov, G., Grunig, G., Koth, L., Solomon, C., Erle, D.J. and Sheppard, D. (2001) Interleukin-13 induces dramatically different transcriptional programs in three human airway cell types. *Am. J. Respir. Cell Mol. Biol.*, **25**, 474–485.
11. Oberhauser, A.F., Marszalek, P.E., Erickson, H.P. and Fernandez, J.M. (1998) The molecular elasticity of the extracellular matrix protein tenascin. *Nature*, **393**, 181–185.
12. Chiquet-Ehrismann, R., Tannheimer, M., Koch, M., Brunner, A., Spring, J., Martin, D., Baumgartner, S. and Chiquet, M. (1994) Tenascin-C expression by fibroblasts is elevated in stressed collagen gels. *J. Cell Biol.*, **127**, 2093–2101.
13. Siri, A., Carnemolla, B., Saginati, M., Leprini, A., Casari, G., Baralle, F. and Zardi, L. (1991) Human tenascin: primary structure, pre-mRNA splicing patterns and localization of the epitopes recognized by two monoclonal antibodies. *Nucleic Acid. Res.*, **19**, 525–531.
14. NIH (1995) Global Initiative for Asthma. *NHLBI Global Strategy for Asthma Management and Prevention NHLBI/WHO Workshop.* NIH publication, Bethesda, MD.
15. Wjst, M., Fischer, G., Immervoll, T., Jung, M., Saar, K., Rueschendorf, F., Reis, A., Ulbrecht, M., Gomolka, M., Weiss, E.H. *et al.* (1999) A genome-wide search for linkage to asthma. German Asthma Genetics Group. *Genomics*, **58**, 1–8.
16. Kaarteenaho-Wiik, R., Kinnula, V., Herva, R., Paakko, P., Pollanen, R. and Soini, Y. (2001) Distribution and mRNA expression of tenascin-C in developing human lung. *Am. J. Respir. Cell Mol. Biol.*, **25**, 341–346.
17. Kaarteenaho-Wiik, R., Kinnula, V.L., Herva, R., Soini, Y., Pollanen, R. and Paakko, P. (2002) Tenascin-C is highly expressed in respiratory distress syndrome and bronchopulmonary dysplasia. *J. Histochem. Cytochem.*, **50**, 423–431.
18. Roth-Kleiner, M., Hirsch, E. and Schittny, J.C. (2004) Fetal lungs of tenascin-C-deficient mice grow well, but branch poorly in organ culture. *Am. J. Respir. Cell Mol. Biol.*, **30**, 360–366.
19. Young, S.L., Chang, L.Y. and Erickson, H.P. (1994) Tenascin-C in rat lung: distribution, ontogeny and role in branching morphogenesis. *Dev. Biol.*, **161**, 615–625.
20. Matlin, A.J., Clark, F. and Smith, C.W. (2005) Understanding alternative splicing: towards a cellular code. *Nat. Rev. Mol. Cell Biol.*, **6**, 386–398.
21. Matsuda, A., Yoshiki, A., Tagawa, Y., Matsuda, H. and Kusakabe, M. (1999) Corneal wound healing in tenascin knockout mouse. *Invest. Ophthalmol. Vis. Sci.*, **40**, 1071–1080.
22. Koyama, Y., Kusubata, M., Yoshiki, A., Hiraiwa, N., Ohashi, T., Irie, S. and Kusakabe, M. (1998) Effect of tenascin-C deficiency on chemically induced dermatitis in the mouse. *J. Invest. Dermatol.*, **111**, 930–935.
23. Nakao, N., Hiraiwa, N., Yoshiki, A., Ike, F. and Kusakabe, M. (1998) Tenascin-C promotes healing of habu-snake venom-induced glomerulonephritis: studies in knockout congenic mice and in culture. *Am. J. Pathol.*, **152**, 1237–1245.
24. Matsuda, A., Tagawa, Y. and Matsuda, H. (1999) TGF-beta2, tenascin, and integrin beta1 expression in superior limbic keratoconjunctivitis. *Jpn. J. Ophthalmol.*, **43**, 251–256.
25. American Thoracic Society. (1962) Chronic bronchitis, asthma and pulmonary emphysema: a statement by the Committee on Diagnostic Standards for Nontuberculous Respiratory Diseases. *Am. Rev. Respir. Dis.*, **85**, 762–768.
26. Fujita, K., Kasayama, S., Hashimoto, J., Nagasaka, Y., Nakano, N., Morimoto, Y., Barnes, P.J. and Miyatake, A. (2001) Inhaled corticosteroids reduce bone mineral density in early postmenopausal but not premenopausal asthmatic women. *J. Bone Miner. Res.*, **16**, 782–787.
27. Ohnishi, Y., Tanaka, T., Ozaki, K., Yamada, R., Suzuki, H. and Nakamura, Y. (2001) A high-throughput SNP typing system for genome-wide association studies. *J. Hum. Genet.*, **46**, 471–477.

INFECTION AND IMMUNITY, July 2005, p. 4088–4097 Vol. 73, No. 7
0019-9567/05/$08.00+0 doi:10.1128/IAI.73.7.4088–4097.2005

Nontoxic Shiga Toxin Derivatives from *Escherichia coli* Possess Adjuvant Activity for the Augmentation of Antigen-Specific Immune Responses via Dendritic Cell Activation

Mari Ohmura,[1,2] Masafumi Yamamoto,[2,3] Chikako Tomiyama-Miyaji,[4] Yoshikazu Yuki,[2,5] Yoshifumi Takeda,[6] and Hiroshi Kiyono[2,5]*

Laboratory for Infectious Immunity, RIKEN Research Center for Allergy and Immunology, 1-7-22 Suehiro-cho, Tsurumi-ku, Yokohama City, Kanagawa 230-0045, Japan[1]; Division of Mucosal Immunology, Department of Microbiology and Immunology, The Institute of Medical Science, The University of Tokyo, 4-6-1 Shirokanedai, Minato-ku, Tokyo 108-8639, Japan[2]; Department of Microbiology and Immunology, Nihon University School of Dentistry at Matsudo, 2-870-1 Sakaecho-Nishi, Matsudo, Chiba 271-8587, Japan[3]; Department of Immunology and Medical Zoology, Niigata University Graduate School of Medical and Dental Sciences, 1-757 Asahimachi-dori, Niigata 951-8510, Japan[4]; Faculty of Human Life Science, Jissen Woman's University, 4-1-1 Osakaue, Hino-shi, Tokyo 191-8510, Japan[6]; and Core Research for Evolutional Science and Technology (CREST), Japan Science and Technology Corporation (JST), Tokyo, Japan[5]

Received 10 February 2005/Returned for modification 23 February 2005/Accepted 8 March 2005

Shiga toxin (Stx) derivatives, such as the Stx1 B subunit (StxB1), which mediates toxin binding to the membrane, and mutant Stx1 (mStx1), which is a nontoxic doubly mutated Stx1 harboring amino acid substitutions in the A subunit, possess adjuvant activity via the activation of dendritic cells (DCs). Our results showed that StxB1 and mStx1, but not native Stx1 (nStx1), resulted in enhanced expression of CD86, CD40, and major histocompatibility complex (MHC) class II molecules and, to some extent, also enhanced the expression of CD80 on bone marrow-derived DCs. StxB1-treated DCs exhibited an increase in tumor necrosis factor alpha and interleukin-12 (IL-12) production, a stimulation of DO11.10 T-cell proliferation, and the production of both Th1 and Th2 cytokines, including gamma interferon (IFN-γ), IL-4, IL-5, IL-6, and IL-10. When mice were given StxB1 subcutaneously, the levels of CD80, CD86, and CD40, as well as MHC class II expression by splenic DCs, were enhanced. The subcutaneous immunization of mice with ovalbumin (OVA) plus mStx1 or StxB1 induced high titers of OVA-specific immunoglobulin M (IgM), IgG1, and IgG2a in serum. OVA-specific $CD4^+$ T cells isolated from mice immunized with OVA plus mStx1 or StxB1 produced IFN-γ, IL-4, IL-5, IL-6, and IL-10, indicating that mStx1 and StxB1 elicit both Th1- and Th2-type responses. Importantly, mice immunized subcutaneously with tetanus toxoid plus mStx1 or StxB1 were protected from a lethal challenge with tetanus toxin. These results suggest that nontoxic Stx derivatives, including both StxB1 and mStx1, could be effective adjuvants for the induction of mixed Th-type $CD4^+$ T-cell-mediated antigen-specific antibody responses via the activation of DCs.

For the design of effective vaccines in the areas of immunology and infectious diseases, a primary focus of research is the development of effective and safe adjuvants, which instruct and control the selective induction of the appropriate type of antigen-specific immune response. Thus far, several bacterial enterotoxins, including the cholera toxin (CT) of *Vibrio cholerae* and the heat-labile enterotoxin (LT) of enterotoxigenic *Escherichia coli*, are known to be potentially strong adjuvants when given by the oral, nasal, or parenteral route (7, 9, 18, 52). As early as 1972, it was reported that CT acts as an adjuvant for antibody responses following intravenous administration (32). The mucosal administration of CT was shown to elicit antigen (Ag)-specific Th2-type $CD4^+$ T-cell responses via high levels of interleukin-4 (IL-4) and IL-5 production, which in turn enhanced Ag-specific systemic immunoglobulin G1 (IgG1) and IgE and mucosal secretory IgA responses (28). In contrast, LT was shown to induce mixed $CD4^+$ Th1- and Th2-type cells producing gamma interferon (IFN-γ), IL-4, IL-5, IL-6, and IL-10, with subsequent serum IgG1 and IgG2a and mucosal secretory IgA responses (47). Other bacterial toxins, such as pertussis toxin and a genetically detoxified derivative of pertussis toxin, PT-9K/129G, have also been shown to possess mucosal adjuvant activities (3, 11, 36). Pertussis toxin potentiates Th1 and Th2 responses to a coadministered antigen (37). The administration of a chimeric molecule composed of the gp120 V3 loop region of the MN strain of human immunodeficiency virus type 1 (HIV-1) and a nontoxic form of *Pseudomonas* exotoxin resulted in strong antigen-specific immune responses to an integrated HIV Ag (30).

It is interesting that in the case of Shiga toxin (Stx), oral administration confers immunogenicity but not adjuvanticity (43). Stx is produced by Stx-producing *E. coli* and is one of the major virulence factors for infectious diseases by Stx-producing *E. coli*. Stx is a holotoxin composed of an approximately 32-kDa A subunit in noncovalent association with a pentameric ring of identical nontoxic B subunits, each of which has a

* Corresponding author. Mailing address: Division of Mucosal Immunology, Department of Microbiology and Immunology, The Institute of Medical Science, The University of Tokyo, 4-6-1 Shirokanedai, Minato-ku, Tokyo 108-8639, Japan. Phone: 81-3-5449-5270. Fax: 81-3-5449-5411. E-mail: kiyono@ims.u-tokyo.ac.jp.

molecular mass of 7.7 kDa. The A subunit is the enzymatic component of the toxin and acts as a highly specific *N*-glycosidase enzyme, hydrolyzing the bond between ribose and a single adenine residue found on a prominent loop structure in the 28S rRNA component of eukaryotic ribosomes (10, 39). The B subunits mediate toxin binding to the membrane-neutral glycolipids glogotriaosylceramid and globotetraosylceramid (38). Stx toxins are classified into the following two groups: Stx1, which is identical to Shiga toxin at the amino acid sequence level, and Stx2, which is immunologically different from Stx1 (42).

In previous studies, we generated E167Q/R170L (mStx1), a double mutant of Stx1 which harbors amino acid substitutions in the RNA *N*-glycosidase active center which were derived by site-directed mutagenesis. mStx1 lacks RNA *N*-glycosidase activity, cytotoxicity, and mouse lethality (33). For the present study, we assessed the capability of mStx1 and StxB1 to provide activation signals to dendritic cells (DCs) and T cells and then addressed the issue of whether this capability of mStx1 and StxB1 is connected to in vivo adjuvanticity when these molecules are subcutaneously coadministered with a protein antigen. The results obtained in this study suggest that both mStx1 and StxB1 act as effective adjuvants for the induction of Ag-specific antibody (Ab) responses via DC activation.

MATERIALS AND METHODS

Mice. C57BL/6 and BALB/c mice were purchased from SLC (Shizuoka, Japan) and were maintained and bred in the experimental animal facilities of Niigata University Graduate School of Medical and Dental Science, the Research Institute for Microbial Diseases, Osaka University, and the Institute of Medical Science, University of Tokyo, under pathogen-free conditions using microisolator cages. DO11.10 T-cell receptor (TCR)-transgenic mice, which recognize the OVA peptide 323-329 in association with I-A^d (31), were kindly provided by Kazuhiko Yamamoto (University of Tokyo, Tokyo, Japan). All mice were provided sterile food and water ad libitum and were maintained in our experimental animal facility. C57BL/6 and BALB/c mice of 8 to 12 weeks of age and DO11.10 Tg mice of 5 to 12 weeks of age were used for this study.

Bacterial toxins. A mutant of Stx1 (mStx1) and native Stx1 (nStx1) were purified from *E. coli* MC 1061 strains M 23 and 87-27, respectively, according to a previously described method (14, 33). Purification steps included ion-exchange chromatography, chromatofocusing, and high-performance liquid chromatography as described previously (14). The B subunit of Stx1 (StxB1) was derived from *Bacillus brevis* pNU212-VT1B and was purified by the use of ion-exchange chromatography and gel filtration (5).

The amounts of endotoxin in the toxin preparations were measured with an Endospec-SP test (Seikagaku Co., Tokyo, Japan). The nStx1, mStx1, and StxB1 preparations contained 7.03 pg, 34.0 pg, and 3.05 pg of lipopolysaccharide (LPS) per 10 μg of protein, respectively. These ranges of LPS contamination have been shown to be ineffective for the stimulation of lymphoid cells (22, 50).

Culture conditions, treatment of BMDCs in vitro, and treatment of BMDCs with Stx1 derivatives. For the generation of bone marrow-derived DCs (BMDCs), male C57BL/6 or BALB/c mice were sacrificed, and their bone marrow was isolated and then flushed from the femur and tibia (12). Erythrocytes were depleted with ammonium chloride. DCs were generated from bone marrow precursors as described previously (12). Following 6 days of incubation in the presence of an optimal dose of granulocyte-macrophage colony-stimulating factor (10 ng/ml), nonadherent cells were collected and used as a source of BMDCs.

BMDCs were cultured at 5×10^5 cells/ml in 24-well plates (Corning, Inc., Corning, N.Y.) in culture medium containing granulocyte-macrophage colony-stimulating factor (10 ng/ml) (12) in the presence or absence of an optimal dose of a Stx1 derivative (1 μg/ml) for 48 h at 37°C. Culture supernatants were collected and frozen at −70°C until assayed for the synthesis of cytokines, including tumor necrosis factor alpha (TNF-α) and IL-12 p70, by enzyme-linked immunosorbent assays (ELISAs) (AN'LYZA immunoassay kit; R&D Systems, Minneapolis, Minn.).

Fluorescence-activated cell sorting analysis. BMDCs were analyzed 48 h after treatment with a variety of toxin derivatives since a preliminary time kinetics study showed that maximum levels of surface antigen expression were achieved and maintained between 24 and 48 h. Cells were analyzed by use of a FACScan cytometer (Becton Dickinson) using the following antibodies from BD Pharmingen and Beckman Coulter, Inc. (Fullerton, Calif.): fluorescein isothiocyanate (FITC)-conjugated anti-mouse CD11c (clone HL3), biotin-conjugated anti-mouse CD80 (clone 16-10A1), biotin-conjugated anti-mouse CD86 (clone GL1), biotin-conjugated anti-mouse I-A^b (clone AF6-120.1), biotin-conjugated anti-mouse CD40 (clone 3/23), and phycoerythrin (PE)-conjugated streptavidin. BMDCs and splenic DCs were characterized with FITC-conjugated anti-mouse CD11b (Mac-1; M1/70), PE-conjugated anti-mouse CD11c (HL3), Cy-chrome-conjugated anti-mouse CD8α (53-6.7), allophycocyanin-conjugated anti-mouse CD4 (RM-4-5), FITC-conjugated hamster anti-mouse CD11c (HL3), and PE-conjugated anti-mouse CD45R/B220 (RA3-6B2).

Purification of TCR-transgenic T cells. T cells were purified from the spleens of naive BALB/c mice expressing a transgenic α/β-TCR specific for peptide 323-329 of ovalbumin (OVA) (31) by magnetic bead-activated cell sorting (MACS) using a $CD4^+$ T-cell purification system with $CD4^+$-specific MACS beads (Miltenyi Biotech, Sunnyvale, Calif.). More than 90% of the resulting T-cell population was $CD4^+$ and expressed the OVA-specific TCR transgene. These purified $CD4^+$ T cells (2×10^6 cells/well) were then cultured in RPMI 1640 plus 10% fetal calf serum (FCS) with toxin derivative-treated DCs (5×10^5 cells/well) and 0.3 μM OVA peptide (ISQAVHAAHAEINEAGR-COOH; Peptide Institute, Inc., Minoh, Osaka, Japan) for 3 days at 37°C. In a preliminary experiment, three different amounts of toxin derivative-treated DCs were tested, and 5×10^5 cells/well consistently provided the most reproducible data. $CD4^+$ T cells were then stimulated with 50 ng/ml phorbol myristate acetate (PMA; Sigma, St. Louis, Mo.) and 500 ng/ml ionomycin (Sigma) overnight. Culture supernatants from the different wells were tested for the synthesis of the cytokines IFN-γ, IL-4, IL-5, IL-6, and IL-10 by ELISAs (AN'LYZA immunoassay kit; R&D Systems).

Induction of T-cell proliferation. BMDCs (1.7×10^4 cells/well) were incubated in round-bottomed 96-well plates (Corning) in the presence of 1 μg of Stx1 derivative for 48 h at 37°C and then were irradiated with 30 Gy of radiation. The plates were extensively washed with RPMI 1640 followed by complete RPMI 1640 containing 10% FCS, HEPES buffer (15 mM), L-glutamine (2 mM), penicillin (100 U/ml), and streptomycin (100 μg/ml). OVA-specific transgenic T cells (5×10^4 cells/well) were added to the DC-coated wells. The plates were then incubated in the presence of 0.3 μM OVA peptide for an additional 3 days at 37°C. [^{3}H]thymidine (0.5 μCi; Amersham Pharmacia Biotech, Buckinghamshire, England) was added to each well 18 h before harvesting, and incorporated radioactivity was then measured with an LS1701 scintillation counter (Beckman Coulter Inc., Hialeah, Fla.). The results are expressed as stimulation indexes (E/C), defined as the ratios between the amounts of [^{3}H]thymidine incorporated into T cells incubated with toxin derivative-treated DCs and the amount of [^{3}H]thymidine incorporated into T cells incubated with untreated DCs.

Isolation of splenic DCs. Spleens were isolated from mice receiving subcutaneous administrations of Stx1 derivatives and were then suspended in RPMI 1640 medium containing 2% FCS, HEPES buffer (15 mM), L-glutamine (2 mM), penicillin (100 U/ml), and streptomycin (100 μg/ml). The spleens were digested with collagenase D (400 Mandl units/ml; Roche, Indianapolis, Ind.) as previously described (45), and then the red blood cells were lysed with ammonium chloride-potassium lysing buffer. Briefly, the spleens were incubated with collagenase D (400 Mandl units/ml) and DNase I (15 μg/ml; Roche) for 35 min at 37°C in RPMI 1640 medium, and EDTA was added to a final concentration of 5 mM during the last 5 min of incubation. For DC enrichment, released cells were layered over a metrizamide gradient column (Accurate, Westbury, N.Y.) (14.5 g of metrizamide added to 100 ml of complete medium) and centrifuged, and the low-density fraction was collected as DCs (26). The enriched DCs were counted and then stained with appropriate monoclonal antibodies as described above for fluorescence-activated cell sorting analysis.

Immunization protocol. A standard subcutaneous immunization protocol was used for this study (55). Mice were subcutaneously immunized on days 0 and 14 with a 100-μl aliquot containing 100 μg of ovalbumin (OVA; Sigma) alone or combined with an optimal dose of mStx1 (10 μg), StxB1 (10 μg), or nStx1 (50 ng) as an adjuvant. This dose of OVA has been shown to be optimal and is routinely used in our laboratory (55). The optimal doses of the Stx1 derivatives were determined in preliminary experiments. In the case of the native form, the dose was selected as the concentration which did not show in vivo toxicity. For an assay of protection against tetanus toxin, mice were subcutaneously immunized on days 0 and 14 with a 100-μl aliquot of tetanus toxoid (TT; 307 μg/ml, 900 limit of flocculation (Lf)/ml, 2,932 Lf/mg PN; provided by Y. Higashi, Osaka University, Biken Foundation, Osaka, Japan) alone or combined with mStx1 (1, 10, or 25 μg) or StxB1 (1, 10, or 25 μg) as an adjuvant.

Analysis of Ag-specific Ab isotype and IgG subclass responses. Ag-specific Ab titers in serum were determined by ELISAs as described previously (28, 51). Briefly, plates were coated with OVA (1 mg/ml) or TT (5 μg/ml) and blocked with 1% bovine serum albumin in phosphate-buffered saline (PBS). After the plates were washed, serial dilutions of serum were added in duplicate. Following incubation, the plates were washed and a peroxidase-labeled goat anti-mouse μ, γ, or α heavy chain-specific Ab (Southern Biotechnology Associates, Birmingham, Ala.) was added to appropriate wells. Finally, 3,3',5,5'-tetramethylbenzidine (TMB) with H_2O_2 was added for color development. For IgG subclass analysis, biotinylated rat monoclonal anti-mouse γ1 (G1-7.3), γ2a (R19-15), γ2b (R12-3), and γ3 (R40-82) heavy chain-specific Abs (Pharmingen) and streptavidin-conjugated peroxidase (Vector Laboratories, Inc., Burlingame, Calif.) were employed. End-point titers were expressed as reciprocal $\log_2$ values of the last dilutions giving optical densities at 450 nm of ≥0.1 above the negative control.

Detection of Ag-specific AFCs. For the elucidation of Ag-specific Ab-forming cells (AFCs), an enzyme-linked immunospot (ELISPOT) assay was employed as previously described in detail (51, 52). Splenic mononuclear cells were resuspended in complete medium. Ninety-six-well nitrocellulose-based plates were coated with 1 mg/ml of OVA diluted in PBS for the enumeration of Ag-specific AFCs. The wells were blocked with complete medium. Cells at various dilutions were added and incubated for 6 h at 37°C in 5% CO_2 in moist air. Antigen-specific AFCs were detected with a peroxidase-labeled anti-mouse μ, γ, or α heavy chain Ab (Southern Biotechnology Associates) and then visualized by adding the chromogenic substrate 3-amino-9-ethylcarbazole (Moss Inc., Pasadena, Md.). Spots were counted with the aid of a dissecting microscope (SZH Zoom stereo microscope system; Olympus, Lake Success, N.Y.).

Analysis of OVA-specific $CD4^+$ T-cell responses. $CD4^+$ T cells were purified from splenic cell suspensions by use of a magnetic bead-activated cell sorter system (Miltenyi Biotech) (51). Splenic mononuclear cells were initially applied to a nylon wool column (Polysciences, Warrington, Pa.) and incubated at 37°C for 1 h to remove adherent cells. Purified $CD4^+$ T cells were then obtained by positive sorting using a magnetic bead separation system consisting of anti-CD4 monoclonal Ab (clone GK1.5)-conjugated microbeads (Miltenyi Biotech). Purified splenic $CD4^+$ T cells (>98% pure) were cultured at a density of 4×10^6 cells/ml with OVA (1 mg/ml), T-cell-depleted, irradiated (30 Gy) splenic feeder cells (8×10^6 cells/ml), and recombinant IL-2 (rIL-2; 10 units/ml) (Pharmingen) in complete medium (51). These $CD4^+$ T-cell cultures were incubated for 3 days at 37°C in 5% CO_2 in air. For measurements of the levels of Ag-specific T-cell proliferation, 0.5 μCi of [^{3}H]thymidine (Amersham Pharmacia Biotech) was added to individual cultures 18 h before termination, and the uptake of [^{3}H]thymidine was determined in counts per minute (cpm) by use of a scintillation counter (55).

Tetanus toxin challenge. Tetanus toxin was diluted in 0.5% gelatin–PBS, and an appropriate lethal dose (130 50% lethal doses [LD_{50}s]) was given subcutaneously to each group of mice as described previously (15, 20). Mice were then monitored daily for paralysis and death.

Statistical analysis. The results are presented as means ± 1 standard error (SE). Statistical significance ($P < 0.05$) was determined by Student's t test and by the Mann-Whitney U test of unpaired samples.

RESULTS

mStx1 and StxB1 up-regulate cell surface expression of costimulatory molecules and MHC class II molecules on BMDCs. On day 6 of bone marrow-derived DC (BMDC) cultures, >90% of the cells were determined to be $CD11c^+$ (data not shown). The CD11b, CD8α, CD4, and B220 cells identified among the BMDCs were characterized as having the $CD11b^+$, $CD8\alpha^-$, $CD4^-$, and $B220^-$ phenotypes, respectively (data not shown). These BMDCs were incubated with or without Stx1 derivatives for 48 h, and the expression of cell surface molecules was analyzed by flow cytometry. Even nonactivated BMDCs showed moderate expression of the costimulatory molecules CD80 (B7-1) and CD86 (B7-2) and of major histocompatibility complex (MHC) class II molecules. The addition of SxtB1 resulted in a moderate up-regulation of CD86, MHC class II, and CD40 expression on BMDCs. Furthermore, StxB1 enhanced the expression of CD80; however, the CD80 level was lower than that of CD86 (Fig. 1).

The expression of CD86, but not that of CD80, was up-regulated when BMDCs were exposed to mStx1. In contrast, nStx1 failed to enhance the expression of these activation molecules on BMDCs. The expression of CD40 on BMDCs was also up-regulated by treatment with mStx1 or StxB1 (Fig. 1). An increase in the expression of these activation molecules also occurred after the treatment of cells with an optimal concentration (1 μg/ml) of LPS (data not shown), a known activator of DCs (17). To exclude any effects of contaminating endotoxins, we incubated BMDCs, with or without Stx1 derivatives, after the pretreatment of Stx1 derivatives with 5 μg/ml polymyxin B. Polymyxin B did not affect Stx1 derivative-induced surface marker expression (data not shown).

Induction of cytokine synthesis by StxB1-treated BMDCs. To analyze whether the observed phenotypic maturation (e.g., the expression of CD80, CD86, and MHC class II) was associated with cytokine production, we tested StxB1- and mStx1-treated BMDCs for an enhancement of TNF-α and IL-12 p70 synthesis. BMDCs incubated with StxB1 for 48 h produced modest amounts of TNF-α and IL-12 (Table 1), which was consistent with the observation of the expression of functional molecules of StxB1-treated BMDCs. In contrast, the incubation of BMDCs with nStx1 and mStx1 failed to invoke any increases in cytokine production. Thus, BMDCs activated by treatment with StxB1 exhibited the most enhanced capacity to secrete cytokines such as TNF-α and IL-12.

Enhanced stimulation of T cells by Stx1 derivative-activated BMDCs. In the next experiment, we tested whether the activation of DCs by mStx1 or StxB1 translated to an increased functional ability of DCs to stimulate T-cell proliferation and subsequent Th1 (IFN-γ) and Th2 (IL-4, IL-5, IL-6, and IL-10) cytokine production. In this assay, Stx1 derivative-stimulated DCs were cocultured with an OVA-specific peptide and splenic T cells isolated from OVA Tg mice. Stx1 derivative-treated BMDCs promoted higher levels of OVA-specific $CD4^+$ T-cell proliferation than did untreated DCs (Fig. 2A), with StxB1-treated BMDCs inducing the highest levels and mStx1-treated BMDCs inducing the next highest levels. In contrast, nStx1-treated BMDCs only weakly enhanced T-cell responses. Similarly enhanced T-cell proliferative responses were also noted when alloreactive responder T cells were cocultured with Stx1 derivative-treated BMDCs (data not shown).

To determine whether the observed increase in OVA-specific $CD4^+$ T-cell proliferation induced by StxB1- or mStx1-treated BMDCs was associated with Th1 and Th2 cytokine production, we harvested culture supernatants and subjected them to IFN-γ-, IL-4-, IL-5-, IL-6-, and IL-10-specific ELISAs. StxB1-treated DCs promoted an increased synthesis of cytokines such as IFN-γ, IL-4, IL-5, IL-6, and IL-10 (Fig. 2B) most effectively, followed by those treated with mStx1 and nStx1 (Fig. 2B). However, it should be pointed out that Stx1 derivatives significantly enhanced only IL-6 synthesis, prompting little or no release of the other cytokines. Among the Stx1 derivatives, StxB1 possessed the most potent immunoenhancing activity for an increase of T-cell proliferation and subsequent Th1 and Th2 cytokine production through the activation of BMDCs.

In vivo effects of mStx1 and StxB1 on the up-regulation of costimulatory molecules and MHC class II on splenic DCs. It

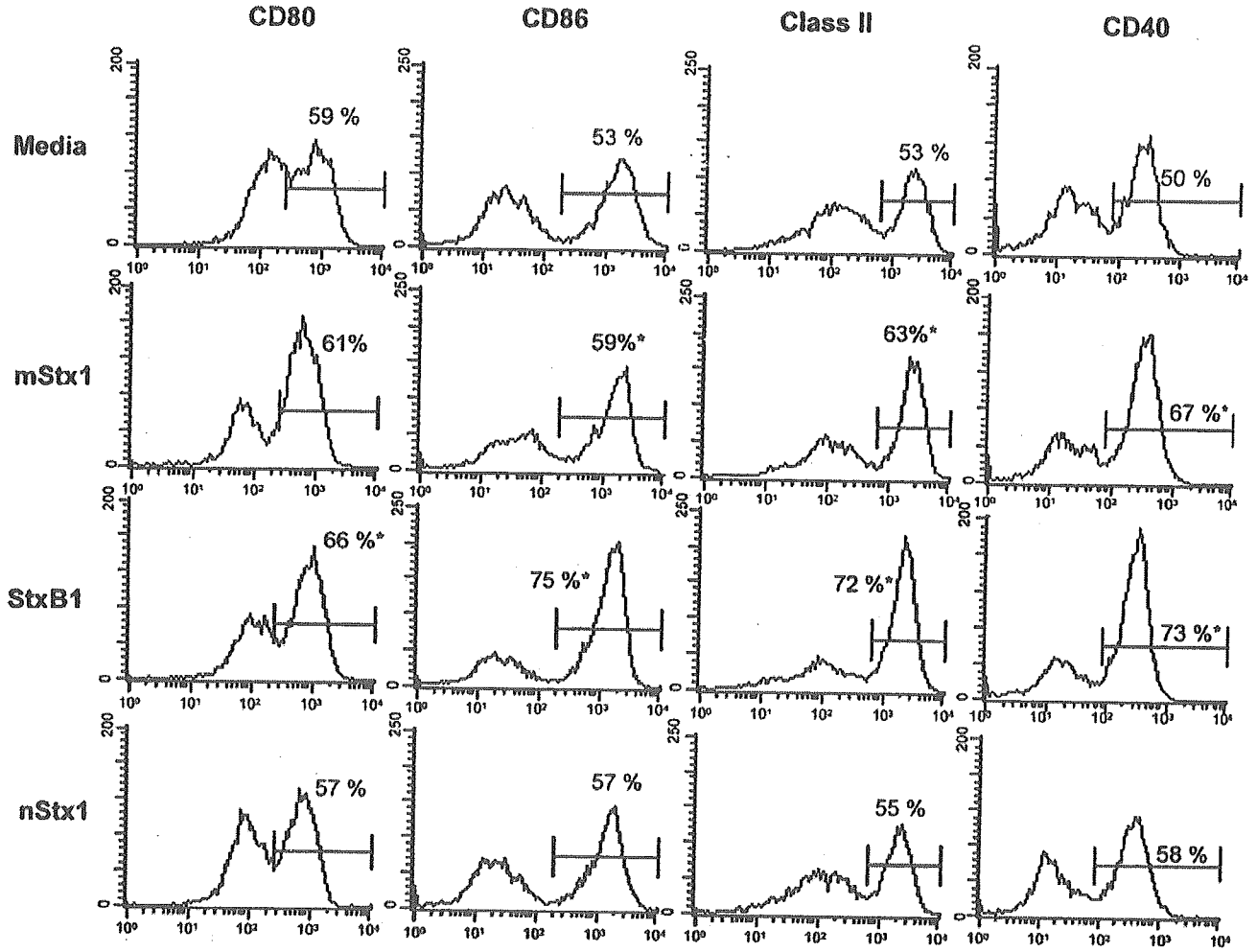

FIG. 1. Effects of StxB1, mStx1, and nStx1 on the expression of CD80, CD86, CD40, and MHC class II by bone marrow-derived DCs (BMDCs). BMDCs were cultured with Stx1 derivatives (StxB1, 1 μg/ml; mStx1, 1 μg/ml; nStx1, 1 μg/ml) for 48 h since a preliminary study showed that the maximum levels of surface antigen expression occurred between 24 and 48 h. Cell surface Ag expression was analyzed by flow cytometry as described in Materials and Methods. The data are presented as histograms and are expressed as means of three independent experiments. The percentage within each panel indicates the number of cells staining strongly for the indicated marker. *, $P < 0.05$ compared with the control medium-treated culture. Data were obtained by using the $CD11c^+$ gated cell fraction.

was important to examine whether in vivo administration of the Stx1 derivatives could modulate DC function. Thus, the expression of costimulatory molecules and MHC class II on splenic DCs was analyzed by flow cytometry 12 h and 48 h after Stx1 derivatives were subcutaneously administered to healthy mice (Table 2).

TABLE 1. TNF-α and IL-12 p70 synthesis by StxB1-, mStx1-, or Stx1-treated murine BMDCs[a]

Stimulator	TNF-α concn (pg/ml)	IL-12 concn (pg/ml)
mStx1	260 ± 81	90 ± 18
StxB1	470 ± 92*	260 ± 34*
nStx1	240 ± 42	76 ± 13
media	280 ± 92	82 ± 14

[a] Culture supernatants were harvested and then analyzed for the production of secreted cytokines by the use of appropriate cytokine-specific ELISAs. The results are expressed as means ± SEM and were taken from a total of three separate experiments. *, $P < 0.05$ compared with a culture to which no stimulator was added.

As shown above for nonactivated BMDCs, the splenic DCs isolated from healthy mice also expressed $CD11b^+$ (data not shown). Nonactivated splenic DCs were also found to naturally express moderate levels of the costimulatory molecules CD80 and CD86, MHC class II, and CD40 (Table 2), whose levels were up-regulated after the administration of StxB1. Interestingly, the up-regulation of CD80 expression was observed as early as 12 h after the administration of StxB1, with the expression of CD86, CD40, and MHC class II appearing 48 h after administration. After a subcutaneous injection of mStx1 into mice, the expression of CD40 and MHC class II was up-regulated. In contrast, as seen with BMDCs, nStx1 failed to enhance the expression of any of these costimulatory molecules, except for MHC class II, on splenic DCs.

Enhancement of Ag-specific Ab responses by subcutaneous immunization of mice with OVA and mStx1 or StxB1. To examine in vivo the immunoenhancing activities of Stx1 derivatives, we subcutaneously immunized mice with an optimal

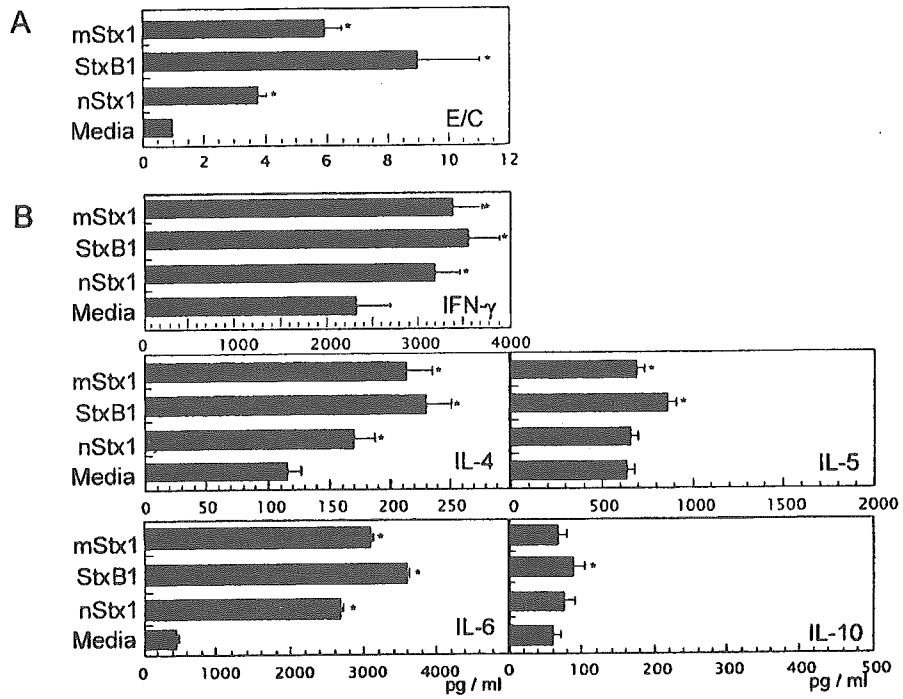

FIG. 2. Activation of OVA-specific $CD4^+$ T-cell responses by Stx1 derivative-treated BMDCs. T-cell proliferation (A) and Th1 and Th2 cytokine production (B) by $CD4^+$ T cells from DO10.11 Tg mice stimulated with Stx1 derivative-treated BMDCs were examined. BMDCs pretreated with 1 μg/ml Stx1 derivative were washed and then cocultured with purified $CD4^+$ T cells (10^6/ml) from DO11.10 Tg mice in the presence of 0.3 μM $OVA_{323-329}$ peptide for 3 days. An aliquot of cell culture was subjected to DNA synthesis by the addition of [^{3}H]thymidine during the last 18 h of incubation. For cytokine analysis, another aliquot of $CD4^+$ T cells was harvested and then treated with 50 nM PMA and 500 nM ionomycin overnight. No or little cytokine release was detected for $CD4^+$ T cells without PMA and ionomycin. The results are expressed as mean E/C ± standard errors of the means (SEM) for triplicate cultures. *, $P < 0.05$ compared with the control medium-treated culture. The count for the control culture was 6,880 ± 380 cpm. The results of the T-cell proliferation assay (A) are expressed as mean E/C (experimental, stimulated value/control, nonstimulated value) ± SEM of triplicate cultures.

dose of OVA in the presence or absence of the toxin derivatives. The coadministration of 10 μg of mStx1 or StxB1 resulted in high levels of OVA-specific IgG, IgM, and IgA (Fig. 3A). In contrast, 50 ng of nStx1 did not support the generation of any isotype of anti-OVA Ab. As one might expect, when mice were immunized with OVA alone, antigen-specific Ab responses were not induced (Fig. 3A). An analysis of antigen-specific IgG antibody-forming cells (AFCs) in the spleens of mice immunized with OVA plus Stx1 derivatives confirmed the results obtained for the characterization of OVA-specific Ab titers in sera. Thus, significant numbers of OVA-specific IgG AFCs were detected in the spleens of mice subcutaneously immunized with OVA plus mStx1 or StxB1 as an adjuvant (Fig. 3B). In contrast, obvious OVA-specific IgG AFCs were not seen in the spleens of mice given OVA alone or OVA plus nStx1 (Fig. 3B). A subsequent analysis of the OVA-specific IgG subclasses revealed that the major antigen-specific IgG subclass response was IgG1, followed by IgG2a, after the coadministration of mStx1 or StxB1 (Fig. 3C). These findings demonstrate that Stx1 derivatives, especially nontoxic forms of StxB1 and mStx1, are potent immunoenhancing molecules in vivo.

Induction of OVA-specific $CD4^+$ Th1- and Th2-cell responses after immunization with OVA and Stx1 derivatives.

TABLE 2. Characterization of CD80, CD86, CD40, and MHC class II expression by mStx1-, StxB1-, or nStx1-treated splenic DCs

Stimulator	% of the highest intensity of the expressed molecule							
	CD80		CD86		CD40		MHC class II	
	12 h	48 h	12 h	48 h	12 h	48 h	12 h	48 h
mStx1	43.0 ± 3.9	16.5 ± 9.3*	43.6 ± 2.9*	45.3 ± 2.5	58.3 ± 5.8*	37.6 ± 1.7	48.8 ± 3.1	65.9 ± 7.5*
StxB1	55.8 ± 2.6*	33.9 ± 1.6*	20.0 ± 4.3*	75.3 ± 14.3*	37.6 ± 1.4*	63.3 ± 4.4*	45.1 ± 2.2*	70.4 ± 6.3*
nStx1	33.2 ± 1.4*	15.7 ± 8.6*	17.4 ± 10.5*	30.2 ± 7.5*	27.4 ± 3.0*	9.7 ± 9.1*	42.5 ± 4.7*	57.3 ± 2.7*
PBS	42.4 ± 1.3	50.9 ± 6.6	49.6 ± 1.7	49.2 ± 6.6	34.7 ± 0.5	37.2 ± 7.5	51.3 ± 2.6	49.2 ± 6.2

Twelve or 48 h after the subcutaneous administration of StxB1 (10 μg/mouse), mStx1 (10 μg/mouse), or nStx1 (50 ng/mouse), mice were sacrificed for the preparation of splenocytes. The cells were then analyzed by flow cytometry. The data are means ± SEM are representative of three independent experiments. *, $P < 0.05$ compared with mice administered PBS.